arXiv:1506.08739v3 [quant-ph] 14 Oct 2015

Bloch Radii Repulsion in Separable Two-Qubit Systems

Paul B. Slater*

University of California,

Santa Barbara, CA 93106-4030

(Dated: January 1, 2024)

Abstract

Milz and Strunz recently reported substantial evidence to further support the previously conjectured separability probability of $\frac{8}{33}$ for two-qubit systems (ρ) endowed with Hilbert-Schmidt measure. Additionally, they found that along the radius (r) of the Bloch ball representing either of the two single-qubit subsystems, this value appeared constant (but jumping to unity at the locus of the pure states, $r = 1$). Further, they also observed (personal communication) such separability probability r-invariance, when using, more broadly, random induced measure ($K = 3, 4, 5, \ldots$), with $K = 4$ corresponding to the (symmetric) Hilbert-Schmidt case. Among the findings here is that this invariance is maintained even after splitting the separability probabilities into those parts arising from the determinantal inequality $|\rho^{PT}| > |\rho|$ and those from $|\rho| > |\rho^{PT}| > 0$, where the partial transpose is indicated. The nine-dimensional set of generic two-re[al]bit states endowed with Hilbert-Schmidt measure is also examined, with similar conclusions. Contrastingly, two-qubit separability probabilities based on the Bures (minimal monotone) measure diminish with r. Moreover, we study the forms that the separability probabilities take as joint (bivariate) functions of the radii (r_A, r_B) of the Bloch balls of *both* single-qubit subsystems. Here, a form of Bloch radii *repulsion* for separable two-qubit systems emerges in *all* our several analyses. Separability probabilities tend to be smaller when the lengths of the two radii are closer. In Appendix A, we report certain companion results for the much-investigated, more analytically amenable (7-dimensional) X-states model.

PACS numbers: Valid PACS 03.67.Mn, 02.50.Cw, 02.40.Ft, 03.65.-w

*Electronic address: slater@kitp.ucsb.edu

Contents

I. Introduction 3

II. Background 4

III. Hilbert-Schmidt Analysis 5

IV. Random Induced Measure Analyses 7

A. The case K=3 7

B. The case K=5 7

V. Bures Analysis 8

VI. Two-Rebit Hilbert-Schmidt Analysis 8

A. Dyson-index relations between rebit and qubit $r_A = r_B$ formulas 9

VII. Division of separability probabilities between $|\rho^{PT}| > |\rho|$ and $|\rho| > |\rho^{PT}| > 0$ 10

A. Hilbert-Schmidt ($K = 4$) case 10

B. Random Induced $K = 3$ case 10

C. Random Induced $K = 5$ case 10

D. Two-rebit case 11

E. Bivariate Extension 11

VIII. Concluding Remarks 11

IX. Appendix A: X-states analyses 14

A. Certain univariate X-states separability probability *conditional* distributions 15

B. Use of Fano correlation parameter $c_{33} = M_{zz}$ 17

C. Random Induced $K = 5$ case 17

D. Random Induced $K = 6$ case 18

E. Random Induced $K = 7$ case 18

F. Random Induced $K = 3$ case 19

X. Appendix B: Separability probabilities as a function of $||\rho - \rho^A \otimes \rho^B||_{HS}$ 19

References 19

Acknowledgments 21

I. INTRODUCTION

A considerable body of diverse evidence–though yet no formal proof–has been adduced strongly indicating that the probability that a generic two-qubit system is separable/unentangled is $\frac{8}{33}$ [1–6] [7, sec. VII] [8, sec. 4]. The probability is computed with respect to the Hilbert-Schmidt (flat/Euclidean) measure [9, 10] on the 15-dimensional convex set of 4×4 density matrices (ρ). Milz and Strunz have recently conducted an analysis further supportive of this conjecture, while injecting an interesting new element [11]. They found that the probability of $\frac{8}{33}$ appears to hold *constant* in the radial direction (r_A) of the Bloch ball/sphere parameterization ($r_A \in [0,1]$, $\theta_A \in [0, 2\pi)$, $\phi_A \in [0, \pi]$)

$$\rho_A = \mathrm{Tr}_B \rho = \tag{1}$$

$$\frac{1}{2}\begin{pmatrix} \cos(\phi_A)\, r_A + 1 & \cos(\theta_A)\sin(\phi_A)\, r_A - i \sin(\theta_A)\sin(\phi_A)\, r_A \\ \cos(\theta_A)\sin(\phi_A)\, r_A + i \sin(\theta_A)\sin(\phi_A)\, r_A & 1 - \cos(\phi_A)\, r_A \end{pmatrix}$$

of either of the qubit subsystems (A, B) of ρ, obtained by the partial tracing over ρ of the complementary subsystem–with a singularity occurring at the pure state boundary, $r_A = 1$ (cf. Fig. 10 below). (At times below, we use the symbol r, to denote interchangeably, r_A or r_B. "The Bloch sphere provides a simple representation for the state space of the most primitive quantum unit–the qubit–resulting in geometric intuitions that are invaluable in countless fundamental information-processing scenarios" [12].)

This same r-invariance phenomenon appeared to hold, in general they found, for $2 \times m$ [qubit-qudit] systems. (For $m > 3$, the probability of having a positive partial transpose was employed [11, Fig. 5].) Further, Milz indicated in a personal communication that for the 2×2 qubit-qubit systems endowed with random induced measure (a function of the dimension K of the ancillary space) [13, 14], r-invariance of these separability probabilities–the values of which can now be directly obtained from equation (2) in [15]–also seems to hold. The (symmetric) case $K = 4$ is equivalent to the Hilbert-Schmidt one.

The work of Milz and Strunz is rather similar in motivation with earlier efforts in which it was sought to describe separability probabilities also as functions of single variables (but

other than the Bloch radius)–namely, the "cross-product ratio" (suggested by work of Bloore [16]), $\frac{\rho_{11}\rho_{44}}{\rho_{22}\rho_{33}}$ [1, 17, 18], and the maximal concurrence over spectral orbits [19] (cf. [20]), and the participation ratio and von Neumann-Renyi entropies [21, Figs. 2b, 4] (cf. App. B below and [6, Figs. 1, 2]). None of the univariate separability functions constructed was of the highly intriguing *constant* form, however. (So, in a sense here, the Bloch radius serves as the extreme antithesis of an entanglement indicator, being entanglement-insensitive apparently.)

In this study, we seek to broaden the investigation of Milz and Strunz by examining the nature of the *joint* (bivariate) distribution of the Hilbert-Schmidt separability probability over the radii (r_A, r_B) of *both* qubit subsystems of ρ (sec. III) (cf. [22, 23]). Further, we examine the use of random induced measure for the Hilbert-Schmidt ($K = 4$)-"neighboring" cases of $K = 3$ and 5 (sec. IV). We will, similarly, examine the separability probability with respect to the Bures measure [10, 24, 25] (sec. V), concluding that–contrastingly–the Bures separability probability is not constant over r, but diminishes with the Bloch radius. Two-re[al]bit [26, 27] Hilbert-Schmidt analyses are included in sec. VI, and an apparent related "Dyson-index" effect in sec. VI A. In sec. VII, we examine how the various separability probabilities change as a function of r when they are subdivided into that part arising from the determinantal inequality $|\rho^{PT}| > |\rho|$ and that from $|\rho| > |\rho^{PT}| > 0$ (cf. [5, 28]). In that setting too, r-invariance appears to hold. Further, we attempted companion analyses for two-quater[nionic]bit systems [2, 4, 27], but encountered certain conceptual/computational issues we have yet to successfully resolve.

Appendix A develops upon the X-states analyses of Milz and Strunz [11, Apps. A, B], finding similar results to those reported in the main body of this paper, while in Appendix B we report some results (not directly pertaining to Bloch radii) based on an entanglement measure of Holik and Plastino [29, eq. (9)].

II. BACKGROUND

Milz and Strunz found numerically-based evidence that the Hilbert-Schmidt *volumes* of the two-qubit systems and of their separable subsystems were both proportional to $(1-r_A^2)^6$ [11, eqs. (23), (30),(31)], with the consequent *constant* ratio of the two (simply proportional) volume functions being the aforementioned separability probability of $\frac{8}{33}$.

For the recently much-investigated "toy" model of X-states [30], occupying a seven-

dimensional subspace of the full fifteen-dimensional space, it was possible for them to *formally* demonstrate that the counterpart volume functions, somewhat similarly, were both again proportional, but now to $(1-r_A^2)^3$ (the square root of the higher-dimensional result). The corresponding (constant, but at $r_A = 1$) separability probability was greater than $\frac{8}{33}$, that is $\frac{2}{5}$ [11, Apps. A, B]. This $\frac{2}{5}$ result was also subsequently proven in [15], along with companion X-states findings for the broader class of random induced measures [13, 14].

However, the joint distributions over the *two* radii in which we are expressly interested here in discerning (either in the X-states and/or full model), do not seem readily derivable, even in the analytical frameworks of those two X-states studies (cf. [31]). So recourse to numerical methods seems indicated. The two *marginal* univariate distributions of the desired joint bivariate *volume* distributions should, of course, be proportional to $(1-r_A^2)^6$ and $(1-r_A^2)^3$ in the full and X-states models, respectively. (In Appendix A, we do succeed in constructing the desired bivariate X-states total and separable volume functions and, hence, the associated separability probability function.)

III. HILBERT-SCHMIDT ANALYSIS

We generated 2,548,000,000 two-qubit density matrices, randomly with respect to Hilbert-Schmidt measure, using the simple (Ginibre ensemble) algorithm outlined in [32, eq. (1)]. For each such matrix, we found the values of r_A and r_B, as well as performed the well-known Peres-Horodecki (determinantal-based [33]) test for separability [34, 35] on the partial transpose of ρ. Then, we discretized/binned the values of the r's obtained to lie in intervals of length $\frac{1}{100}$. Thus, we have two 100×100 matrices of counts (which we symmetrize for added stability). In Figs. 1 and 2, we show the histograms of these two sets of counts (cf. [11, Fig. 3]). (Of the 10,000 bins, 9,364 of the total and 9,199 of the separable ones are occupied.)

The first (*total* counts) plot appears to be somewhat broader in nature than the second (*separable* counts) plot, while appearing qualitatively rather similar.

A natural null (product/independence) hypothesis to adopt to explain the nature of Figs. 1 and 2–in light of the assertions of Milz and Strunz [11]–is that both these surfaces are proportional (taking into account the spherical area formula) to $16\pi^2 r_A^2 r_B^2 (1-r_A^2)^6 (1-r_B^2)^6$. As tests of these hypotheses, we show the residuals from the two figures based on such

a prediction (Figs. 3 and 4). The product function just shown was normalized so as to minimize the sum of squares of the residuals. We note, interestingly, that both sets of residuals are bimodal in nature. We can somewhat improve the fits (more so, in the total count case) by employing as the hypothesized form $16\pi^2 r_A^2 r_B^2 \frac{(1-r_A^2)^8(1-r_B^2)^8}{(1-r_A^2 r_B^2)^{13}}$.

In Fig. 5, we show the estimated separability probabilities (the ratio of the second of our plots to the first)–which are clearly now, in contrast to the univariate case–*not* uniform over their (unit square) domain of definition. (Let us note that the associated 100×100 matrix can be considered as an estimate–up to proportionality [here $\frac{8}{33}$]–of a *doubly-stochastic* matrix [36]. Of course, individual bin-ratios of the form $\frac{0}{0}$ are not incorporated into the plot computations throughout this paper.) The main motivation for this study was to discern the functional nature of this surface (Fig. 5).

In Fig. 6, for ease of visualization purposes, we perform a $\frac{\pi}{4}$ rotation of the last figure (cf. [37, eq. (7)]).

In Fig. 7 we present the $r_A = r_B$ cross-section of Fig. 5, and indicate a closely-fitting model for it. For this curve, the total volume–forming the denominator of the separability probability curve–appears to be proportional to $(1-r)^8(1+8r)$, and the numerator comprised of the separable volume to be proportional $(1-r)^9(1+\frac{17}{2}r+29r^2)$, leading to a factor of $(1-r)$ in the equation of the curve. The sample separability probability for those states for which $r_A = r_B$ was recorded as 0.22753675.

In Fig. 8, we show the $r_A + r_B = 1$ (U-shaped) cross-section. A joint plot of these two curves is given in Fig. 9. (Let us observe that the four Bell states are themselves unpolarized, that is $r_A = r_B = 0$, *and* maximally entangled (cf. [38]).)

The estimated separability (marginal) probabilities over either one of the Bloch radii are shown in Fig. 10, along with a 95% confidence interval (based on the suitable large-sample normal distribution approximation to the binomial distribution) about the conjectured value of $\frac{8}{33} \approx 0.242424$. (The sample estimate of this probability that we obtained here was 0.242425003.) This plot helps to confirm the chief (r-invariance) 2×2 findings of Milz and Strunz.

IV. RANDOM INDUCED MEASURE ANALYSES

We explore the questions raised above, but now in the broader context of random induced measure [10, 13, 14], involving the use of the natural, rotationally invariant measure on the set of all pure states of a $4 \times K$ composite system. By tracing over the K-dimensional ancillary system, one obtains the two-qubit states that we will analyze. We generate random matrices with respect to these measures using the algorithm specified in [39] (cf. [40]).

A. The case K=3

Setting $k = K - 4 = -1$, in equation (2) of our recent study [15],

$$P_k^{qubit} = 1 - \frac{3\ 4^{k+3}(2k(k+7)+25)\Gamma\left(k+\frac{7}{2}\right)\Gamma(2k+9)}{\sqrt{\pi}\Gamma(3k+13)}, \tag{2}$$

we obtain that the associated separability probability for this scenario is $\frac{1}{14} \approx 0.0714285$. The related figures–based on 764,000,000 randomly generated 4×4 density matrices–are Figs. 11 to 17, with the sample separability probability estimate being 0.0714333.

For the $r_A = r_B$ curve (Fig. 14), the total volume–forming the denominator of the separability probability curve–appears to be proportional to $(1-r)^5$, and the numerator comprised of the separable volume to contain a factor $(1-r)^6$, leading–again–to a factor of $(1-r)$ in the equation of the curve. The sample separability probability for those states for which $r_A = r_B$ was recorded as $\frac{3396373}{53960055} \approx 0.0629424$.

For the $r_A + r_B = 1$ curve (Fig. 15), an attempt of ours to compute the equation of this curve by taking the ratio of volumes yielded

$$p_{K=3}(r_A + r_B = 1) = \begin{cases} -0.275109 r_A + \frac{0.00894993}{1-r_A} + 0.174492 & 0 < r_A < \frac{1}{2} \\ -0.100617 + 0.275109 r_A + \frac{0.00894993}{r_A} & \frac{1}{2} < r_A < 1 \end{cases} \tag{3}$$

B. The case K=5

Now, inserting $k = 1$ into the two-qubit random-induced formula (2) above, we obtain the associated separability probability for this scenario, $\frac{61}{143} \approx 0.426573$. The related figures are Figs. 18 to 24. These are based on 1,267,000,000 randomly generated density matrices. The estimated separability probability is 0.426549.

For the $r_A = r_B$ curve (Fig. 21), the total volume–forming the denominator of the separability probability curve–appears to be proportional to $(1-r)^{11}(1+11r+40r^2)$, and the numerator comprised of the separable volume to contain a factor $(1-r)^{12}$, leading, again, to a factor of $(1-r)$ in the equation of the curve.

V. BURES ANALYSIS

Our analyses now are based on 424,000,000 randomly generated 4×4 density matrices with respect to the Bures (minimal monotone) measure [10, 24], using the algorithm given in [32, eq. (4)]. We present a series of figures (Figs. 25-31) paralleling those above (Figs. 1-2, 5-10) for the Hilbert-Schmidt measure. Fig. 31 indicates that the separability probability in the radial direction of either reduced qubit subsystem is not constant, but diminishes with r, in strong contrast to the cases analyzed above. The estimate of the Bures separability probability [6, 41, 42] itself that we obtain is 0.0733096.

A "silver mean" conjecture for this last value, that is $\frac{1680\sigma_{Ag}}{\pi^8} \approx 0.0733389$, where the silver mean is defined as $\sigma_{Ag} = \sqrt{2}-1$, had been advanced in [42, eq. (16)]. Clearly, however, the supporting case for this decade-old Bures two-qubit separability probability conjecture is not nearly as strong as is the multifaceted case that has been accumulating in the past few years for the corresponding Hilbert-Schmidt conjecture of $\frac{8}{33}$ [1–5].

VI. TWO-REBIT HILBERT-SCHMIDT ANALYSIS

We have been noting that a remarkably strong, diverse body of evidence [1–6]–though yet no formal proof (cf. [15])–has been accumulating in the past several years for the proposition that the Hilbert-Schmidt separability probability of generic (15-dimensional) two-qubit states is $\frac{8}{33} \approx 0.242424$. Accompanying these results has also been evidence that the Hilbert-Schmidt separability probability of generic (9-dimensional) two-re[al]bit states [26, 27] is $\frac{29}{64} \approx 0.453125$.

In Figs. 32-38 we present a parallel set of figures to those above for 4×4 density matrices with real entries with respect to Hilbert-Schmidt measure. (We follow the prescription given in [32, p. 7] regarding the generation of such random matrices, of which we generate 2,751,000,000.) The separability probability estimate that we obtain is 0.453115. In this

case, each Bloch radius has a two-dimensional, rather than three-dimensional character (nor one-dimensional aspect, as in the X-states).

The two 100×100 matrices of total counts in the Hilbert-Schmidt two-rebit analysis (Fig. 32) and in the Hilbert-Schmidt two-qubit analysis (Fig. 1) have 8,325 of the 10,000 cells both of size at least 100. The correlation between the estimated separability probabilities for those two sets of 8,325 cells was 0.987954. On the other hand, if we first square the values of the two-rebit separability probabilities–as random matrix (Dyson-index) theory [43] might suggest–the correlation is slightly higher, 0.989462.

A. Dyson-index relations between rebit and qubit $r_A = r_B$ formulas

In Fig. 39 we plot the ratio of the estimated two-qubit $r_A = r_B$ probability distribution to the *square* of its two-rebit counterpart. We see that this ratio appears to hold quite constant at roughly $\frac{5}{4}$. This ratio is also, clearly, formally a ratio ($R = \frac{R_{sep}}{R_{tot}}$) of two auxiliary quantities. The numerator R_{sep} is itself the ratio of the two-qubit separable volume to the square of the two-rebit separable volume, and the denominator R_{tot}, likewise in terms of total volumes. Our well-fitting estimates of R_{sep} were $0.0023976r + 0.019464$ and of R_{tot}, $0.0023868r + 0.0171397$, respectively. So, the slopes of the two lines are extremely close, yielding–*via* the equivalence $\frac{R_{sep}}{R_{tot}}$–the near flatness of Fig. 39.

Along such "Dyson-index" lines of thought, we have been investigating–with some numerical encouragement–the possibility that in the $r_A = r_B$ scenarios in the two-rebit case the volume functions might have factors of $(1-r)^4$ and $(1-r)^{\frac{9}{2}}$ in the total and separable cases, respectively. Such an investigation stemmed from the apparent occurrences, noted above, of factors $(1-r)^8$ and $(1-r)^9$ in the two-qubit counterpart volume functions–which appear to be, in full, proportional to $(1-r)^8(1+8r)$ and $(1-r)^9(1+\frac{17}{2}r+29r^2)$.

We would anticipate that related patterns would continue to hold in the case of two-quater[nionic]bits.

VII. DIVISION OF SEPARABILITY PROBABILITIES BETWEEN $|\rho^{PT}| > |\rho|$ AND $|\rho| > |\rho^{PT}| > 0$

It now appears that, in general, for the two-qubit states endowed with random induced measure, the separability probabilities are constant along either Bloch radius (except at the isolated point $r = 1$) of the reduced single-qubit states (Figs. 10, 17, 24). An interesting supplementary question is what are the contributions to the separability probabilities arising from the determinantal inequality $|\rho^{PT}| > |\rho|$ and, complementarily, from $|\rho| > |\rho^{PT}| > 0$.

A. Hilbert-Schmidt ($K = 4$) case

We know from preceding work [5, Table IV] [28] that in the Hilbert-Schmidt case, the conjectured probability of $\frac{8}{33}$ appears to be evenly divided, with each inequality contributing $\frac{4}{33}$. In a further analysis conducted here, based on 1,419,000,000 random matrices, it appears that this amount of $\frac{4}{33} \approx 0.121212$ (the sample estimate being 0.121208) is–paralleling the Milz-Strunz finding for the total (undivided, that is $|\rho^{PT}| > 0$) separability probability–*constant* along the Bloch radius of either reduced single-qubit system (Fig. 40).

B. Random Induced $K = 3$ case

For the $K = 3$ ($k = -1$) case, the entire separability probability of $\frac{1}{14}$ is associated with the inequality $|\rho^{PT}| > |\rho|$, so no similar *nontrivial* splitting can take place. (In this scenario, ρ *must* possess at least one zero eigenvalue, and hence $|\rho| = 0$, thus explaining this phenomenon.)

C. Random Induced $K = 5$ case

For the $K = 5$ ($k = 1$) case, the total separability probability appears–as already noted (sec. IV B)–to be $\frac{61}{143} \approx 0.426573$. Table IV of [5] asserts that the *proportion* of this associated with $|\rho^{PT}| > |\rho|$ is $\frac{45}{122}$, giving us $(\frac{61}{143})(\frac{45}{122}) = \frac{45}{286} \approx 0.157343$. In Fig. 41, we show–based on 1,267,000,000 random matrices–an associated flat-like plot, conforming closely to this value (the overall sample estimate being 0.157323). Thus, it appears that this separability (sub-)probability–and, of course, its complement of $\frac{61}{143} - \frac{45}{286} = \frac{7}{26}$–is constant along either

Bloch radius. So, these analyses serve as an expansion–and a type of further validation–of the Milz-Strunz findings [11].

D. Two-rebit case

In Fig. 42 we present the Hilbert-Schmidt two-rebit counterpart of these several figures, with the sample estimate of the overall separability probability of $\frac{29}{128} \approx 0.226563$, being 0.226554.

E. Bivariate Extension

Additionally, if we similarly split the three *bivariate* separability probability plots (Figs. 5, 20, 34) in accordance with the two determinantal inequalities, the resultant plots appear alike in shape to the parent plots. So, we can certainly conjecture a similar equal splitting of probability phenomenon in that higher-dimensional domain.

VIII. CONCLUDING REMARKS

All the bivariate separability probability estimates presented (Figs. 5, 13, 20, 27, 34) appear to have a saddle point at $(\frac{1}{2}, \frac{1}{2})$, or somewhere in the neighborhood thereof, with the $r_A = r_B$ curves (Figs. 7, 14, 21, 28, 35), possibly achieving their maxima at $r_A = r_B = \frac{1}{2}$ and the $r_A + r_B = 1$ curves (Figs. 8, 15, 22, 29, 36) attaining their minima there. (We have also speculated/conjectured that the various *bivariate* distributions displayed–other than the Bures–are simply proportional to one another, as we and Milz and Strunz have shown appears to be the case with their univariate marginal distributions.) A simple probability distribution over $[0, 1]^2$ with such a saddle point property, that, in addition, has the required marginal univariate *uniform* distributions over r_A or r_B, is

$$p(r_A, r_B) = 2r_A + 2r_B - 4r_A r_B. \tag{4}$$

(This functional form was suggested by Brian Tung in response to a Math Stack Exchange question https://math.stackexchange.com/questions/1271549/bivariate-probability-distributions-over-unit-square-uniform-marginals-midpo.) In Fig. 43 we show the residuals

obtained by subtracting $\frac{8p(r_A,r_B)}{33}$ from the estimated two-qubit Hilbert-Schmidt separability probabilities of Fig. 5.

We were able to obtain a somewhat superior fit (also satisfying the marginal constraints) to this one–as measured by the sum of absolute values of residuals–using a higher-degree form of probability distribution over the unit square, namely

$$p'(r_A, r_B) = \frac{3}{2} r_A^2 r_B + \frac{3}{2} r_A r_B^2 - 6 r_A r_B - \frac{3 r_A^2}{4} + \frac{5 r_A}{2} - \frac{3 r_B^2}{4} + \frac{5 r_B}{2}. \tag{5}$$

Another approach of distinct interest to such fitting is to employ the notion of a "copula"–in particular, that of an Ali-Mikhail-Haq (AMH) copula (parameterized by $\theta \in [-1, 1]$) [44, sec. 3.3.2] [45, 46]. This is particularly useful since it yields a doubly-stochastic measure–in rational function form (unlike most other copula forms)–over $[0, 1]^2$, while our 100×100 matrices of separability probabilities should be–within sampling error-proportional (in terms of the total separability probability constant) to doubly-stochastic matrices. Implementation of this approach (utilizing related Mathematica routines) yielded, *via* maximum-likelihood estimation–the (symmetric in r_A and r_B) function–corresponding (approximately) to $\theta = -\frac{51}{200}$–

$$p''_{2-qubits}(r_A, r_B) = -\frac{1600 \left(51 r_A \left(149 r_B + 251\right) + 251 \left(51 r_B - 251\right)\right)}{33 \left(51 r_A \left(r_B - 1\right) - 51 r_B + 251\right)^3}. \tag{6}$$

The correlation between r_A and r_B in this model is -0.0419873.

Pursuing a parallel approach in the two-rebit case, maximum-likelihood estimation yielded a result close to $v = -\frac{13}{100}$, giving

$$p''_{2-rebits}(r_A, r_B) = -\frac{29 \left(1 - \frac{13}{100} \left(r_A r_B - \frac{13}{100} \left(r_A - 1\right) \left(r_B - 1\right) + r_A + r_B - 2\right)\right)}{64 \left(-\frac{13}{100} \left(r_A - 1\right) \left(r_B - 1\right) - 1\right)^3}. \tag{7}$$

The correlation between r_A and r_B in this model is -0.0800287. In the random induced $K = 3$ setting, our estimate of θ was close to $-\frac{31}{50}$, and for $K = 5$, close to $-\frac{9}{100}$. (It would be of interest to extend the AMH copula framework to multiparameter settings [cf. [47]].)

From Figs. 9, 16, 23, 30 and 37 we see a form of Bloch radii *repulsion*. That is, separability probabilities tend to increase as the gap in value between the lengths of the two radii increase.

At this point, we have not yet achieved our motivating goal in undertaking this study, that is, to determine the precise nature of the bivariate distributions over the pair of Bloch radii. (An area for additional research is to view the desired bivariate separability probabilities in light of the literature on *doubly-stochastic measures* [48].)

A remaining related case that is still not successfully analyzed is that of the 27-dimensional set of generic two-quat[ernionic]bits [27], for which the Hilbert-Schmidt separability probability appears to be $\frac{26}{323} \approx 0.0804954$ [2, 4]. An interesting question here is how to determine the corresponding "Bloch radii" for randomly generated two-quaterbit states (cf. [49]). Further, we have not yet developed a computationally feasible (Mathematica-implemented) algorithm for the random generation of such matrices (cf. [32, 39] [50, Fig. 1]).

Let us note that the two reduced qubit systems of a *pure* two-qubit system must have their Bloch radii equal (totally "non-repulsive"). The separable pure two-qubit systems form a four-dimensional submanifold of the six-dimensional manifold of pure two-qubit systems [10, p. 368], and thus are of relative measure/probability zero. (These observations, it would seem, at least in an informal qualitative manner, are not inconsistent with our general set of results.) In terms of the two-qubit states having only two distinct nondegenerate eigenvalues, Scutaru has shown that "the Bloch vectors of the corresponding qubits are related by a rotation" [51].

In Table I we present the results of an auxiliary set of analyses. Five million random density matrices were generated for each scenario indicated, and the correlation computed between the lengths of the corresponding Bloch radii, both for all the density matrices generated, and also just for the subset of separable density matrices. The consistently smaller correlations for the separable states are a manifestation of the repulsion effect we have documented in this study. (We note, however, that none of these correlations is negative. So, perhaps rather than the term "repulsion", the use of "relative repulsion" or "diminished attraction" might be more strictly appropriate.) Obviously, the correlations in the table based on the Bures measure are exceptionally large.

scenario	all states	separable states
Random Induced $K = 5$	0.145496	0.0968024
Hilbert-Schmidt two-qubits	0.183026	0.107762
Hilbert-Schmidt two-rebits	0.176898	0.118049
Random Induced $K = 3$	0.248993	0.125835
Bures two-qubits	0.388250	0.210838

TABLE I: Correlations between pairs of Bloch radii for all states and all separable states for differing scenarios

Evidence adduced by Milz and Strunz indicated that both the Hilbert-Schmidt total and separable univariate volume functions of two-qubit states were simply proportional to $(1 - r^2)^6$ [11, eq. (23)]. We ourselves fit a function of the form $c(1 - r^2)^p$ to the large sample of such states employed above (sec. III), and obtained estimates of 5.99965 and 5.99926, respectively, of this exponent for the two volumes. Similarly, for the two-rebit set of analyses (sec. VI), the estimates were 6.00439 and 6.00447. For random-induced measure with $K = 3$ (sec. IV A), 3.99973 and 4.00015 were obtained, while for the case $K = 5$ (sec. IV B), the corresponding results were 7.99923 and 7.99917. (A parallel exercise based on the Bures measure [sec. V] yielded the rather proximate results of 3.48845 and 3.58319, respectively.)

Following the work of Braga, Souza and Mizrahi [37, eq. (7)] it might prove advantageous in our quest to model the various bivariate total and separable volume and probability functions discussed above, to employ transformed variables of the form $u_+ = \frac{r_A + r_B}{2}$ and $u_- = \frac{r_A - r_B}{2}$. In fact, this appears to be the case in the following appendix devoted to X-states analyses.

IX. APPENDIX A: X-STATES ANALYSES

We employed the X-states parametrization and transformations indicated by Braga, Souza and Mizrahi [37, eqs. (6), (7)]. Based on these, we were able to reproduce the Hilbert-Schmidt univariate volume result of Milz and Strunz [11, eq. (20), Fig. 1],

$$V_{HS}^{(X)}(r) = \frac{\pi^2}{2304}(1 - r^2)^3, \tag{8}$$

as the marginal distribution (over either r_A or r_B) of the *bivariate* distribution (Fig. 44)

$$ {}_{tot}V_{HS}^{(X)}(r_A, r_B) = \tag{9}$$

$$\begin{cases} -\frac{1}{960}\pi^2 \left(r_A-1\right)^3 \left(r_A \left(r_A+3\right)-5r_B^2+1\right) & r_A > r_B \\ -\frac{1}{960}\pi^2 \left(r_B-1\right)^3 \left(-5r_A^2+r_B \left(r_B+3\right)+1\right) & r_A < r_B. \end{cases}$$

To now obtain the desired X-states bivariate separability probability distribution (perhaps suggestive of the full 15-dimensional counterpart), we find the separable volume counterpart to (9) (Fig. 45)

$$ {}_{sep}V_{HS}^{(X)}(r_A, r_B) = \tag{10}$$

$$\begin{cases} -\frac{\pi^2(r_A-1)^3\left(5(r_A+3)r_B^4-10(3r_A+1)r_B^2+8r_A^2+9r_A+3\right)}{7680} & r_A > r_B \\ -\frac{\pi^2(r_B-1)^3\left(5r_A^4(r_B+3)-10r_A^2(3r_B+1)+r_B(8r_B+9)+3\right)}{7680} & r_A < r_B, \end{cases}$$

and take their ratio (Fig. 46) (noting the cancellation of the $(r-1)^3$-type factors),

$$ p^{X-states}(r_A, r_B) = \tag{11}$$

$$\begin{cases} \frac{5(r_A+3)r_B^4-10(3r_A+1)r_B^2+8r_A^2+9r_A+3}{8\left(r_A(r_A+3)-5r_B^2+1\right)} & r_A > r_B \\ \frac{5r_A^4(r_B+3)-10r_A^2(3r_B+1)+r_B(8r_B+9)+3}{8\left(-5r_A^2+r_B(r_B+3)+1\right)} & r_A < r_B \end{cases}.$$

(Numerical integration of this function over $[0,1]^2$ yielded 0.381678.) Also, Fig. 47 shows the (lower) $r_A = r_B$ and (upper) $r_A + r_B = 1$ cross-sections of Fig. 46. (We note in the next section immediately below an exception to the "repulsion" phenomenon apparently repeatedly appearing above. We computed the correlation between the pair of Bloch radii to be $1 - \frac{11206656}{37748736-10080\pi^2+\pi^4} \approx 0.702341$ for all states and only slightly less, $1 - \frac{74649600}{235929600-25200\pi^2+\pi^4} \approx 0.68326$, for the separable X-states.)

In light of the X-state results (9) and (10), we might speculate that the counterpart bivariate total and separable volumes for the 15-dimensional set of two-qubits states will both consist of the product of $(1-r)^6$ and certain polynomials. The corresponding separability probability function (cf. Fig. 5) would then be a rational one.

A. Certain univariate X-states separability probability *conditional* distributions

The analytic form of the $r_A = r_B$ X-states separability probability curve is

$$p^{\{X-states\}}(r_A = r_B) = -\frac{(r-1)(5r(r(r+5)+3)+3)}{32r+8}. \tag{12}$$

The value of this X-states separability probability function at $(\frac{1}{2},\frac{1}{2})$ is $\frac{139}{384}=\frac{139}{2^7\cdot 3}$, at $(0,0)$ it is $\frac{3}{8}$, and at (1,1) it is 0. The maximum of the $r_A=r_B$ curve is achieved at the positive root ($r\approx 0.2722700792$) of the cubic equation $3r^3+9r^2+r-1=0$, its value there (≈ 0.393558399) being the positive root of the cubic equation $54r^3+108r^2-28r-9=0$. On the other hand, the minimum ($\frac{139}{384}\approx 0.361979$) of the $r_A+r_B=1$ curve

$$p^{\{X-states\}}(r_A=1-r_B)=\begin{cases}-\frac{(r_A-2)r_A\left(5r_A\left(r_A^2+r_A-10\right)+28\right)+8}{8(r_A(4r_A-13)+4)} & 2r_A>1\\ \frac{r_A(r_A(5r_A((r_A-4)r_A-6)+32)+25)-20}{8(r_A(4r_A+5)-5)} & 2r_A<1\end{cases} \tag{13}$$

is attained more simply at $r_A=r_B=\frac{1}{2}$. The maximum of $\frac{1}{2}$ is situated at $r_A=r_B=0$ or 1. So, at least in this model there does not seem to be a corresponding *minimax* result. (Let us very interestingly note that in the interval $r\in[0.40182804,\frac{1}{2}]$ the $p^{\{X-states\}}(r_A=1-r_B)$ curve is dominated by the $p^{\{X-states\}}(r_A=r_B)$ curve. The maximum gap of 0.0056796160 is attained at $r=0.4564893379$. So, at least in this particular scenario, the "repulsion phenomenon" does not fully hold.)

Further, setting $r_B=\frac{1}{2}$, we have

$$p^{\{X-states\}}(r_B=\frac{1}{2})=\begin{cases}\frac{r_A(128r_A+29)+23}{32(4r_A(r_A+3)-1)} & \frac{1}{2}<r_A<1\\ \frac{35r_A^4-50r_A^2+19}{44-80r_A^2} & 0<r_A<\frac{1}{2}\end{cases}. \tag{14}$$

Putting $r_B=0$, we obtain

$$p^{\{X-states\}}(r_B=0)=\frac{r_A\left(8r_A+9\right)+3}{8\left(r_A\left(r_A+3\right)+1\right)}, \tag{15}$$

and with $r_B=1$,

$$p^{\{X-states\}}(r_B=1)=0. \tag{16}$$

It certainly appears that this last result is in direct contradiction with certain assertions of Milz and Strunz: "The latter fact that $p_{sep}^{(X)}(1)=1$ is clear: a pure reduced state ($r=1$) can only be realized by a product and thus, a separable total state" [11, p. 8] (see also the discussion prior to their eq. (23)). We anticipate an eventual clarification of this apparent conflict, possibly in terms of differing dimensionalities of the measures employed.

If we restrict the X-states to those for which $r_A=r_B$, then the separability probability for this continuum $r_A\in[0,1]$ of states is $\frac{8}{21}$. For those for which $r_A=1-r_B$, the corresponding separability probability is $\frac{58}{147}$.

B. Use of Fano correlation parameter $c_{33} = M_{zz}$

In their X-state studies, both Milz and Strunz [11] and Braga, Souza and Mizrahi [37] employ the well-known Fano parameterization of two-qubit systems [52]. Milz and Strunz denote the Fano correlation parameter in the (conventionally denoted) $z-$ or x_3-direction by c_{33}, while Braga, Souza and Mizrahi employ the notation M_{zz}. (The alignments of the Bloch radii–r_A and r_B–are along this same direction in the X-states model, we interestingly note.) Focusing on this parameter yields a number of analytic results, such as the associated X-states separability probability (Fig. 48). (Numerical integration of this function over [-1,1] yielded 0.416283.)

C. Random Induced $K = 5$ case

We have found here–introducing a factor of $|\rho|$ into the integrations in the previously-conducted Hilbert-Schmidt X-states analyses–that the total volume bivariate distribution for the induced measure case of $K = 5$ equals

$$ {}_{tot}V^{(X)}_{K=5}(r_A, r_B) = \tag{17}$$

$$\begin{cases} -\frac{\pi^2 (r_A-1)^5 \left(-6 r_A (r_A+5) r_B^2+r_A (r_A+1)(r_A (r_A+4)+5)+21 r_B^4-6 r_B^2+1\right)}{1290240} & r_A > r_B \\ -\frac{\pi^2 (r_B-1)^5 \left(-6 r_A^2 (r_B (r_B+5)+1)+21 r_A^4+r_B (r_B+1)(r_B (r_B+4)+5)+1\right)}{1290240} & r_A < r_B \end{cases}.$$

The total volume itself is $\frac{\pi^2}{9979200} \approx 9.8901759 \cdot 10^{-7}$. The marginal distributions of the total volume bivariate distribution (17) are of the (again, proportional to $\pi^2(1-r^2)^n$) form

$$V^{(X)}_{K=5}(r) = \frac{\pi^2 (1-r^2)^5}{3686400} = \frac{\pi^2 (1-r^2)^5}{2^{14} \cdot 3^2 \cdot 5^2}. \tag{18}$$

The separable volume is given by

$$ {}_{sep}V^{(X)}_{K=5}(r_A, r_B) = \tag{19}$$

$$\begin{cases} -\frac{\pi^2 (r_A-1)^5 \left(-21 (r_A+5) r_B^6+63 (5 r_A+1) r_B^4-27 r_A (8 r_A+5) r_B^2+r_A (8 r_A (r_A+2)(r_A+3)+25)-27 r_B^2+5\right)}{10321920} & r_A > r_B \\ -\frac{\pi^2 (r_B-1)^5 \left(-21 r_A^6 (r_B+5)+63 r_A^4 (5 r_B+1)-27 r_A^2 (r_B (8 r_B+5)+1)+25 r_B+8 r_B^2 (r_B+2)(r_B+3)+5\right)}{10321920} & r_A < r_B \end{cases}.$$

Its marginal distributions are of the form

$$ {}_{sep}V^{(X)}_{K=5}(r) = \frac{\pi^2 (1-r^2)^5}{5734400} = \frac{\pi^2 (1-r^2)^5}{2^{15} \cdot 5^2 \cdot 7}. \tag{20}$$

The separability probability we found was $\frac{9}{14} \approx 0.642857$–a result also derivable from a formula [53, p.13],

$$\Pr\{|\rho^{PT}| > 0\} = 1 - \frac{2\Gamma(2k+4)^2}{\Gamma(k+2)\Gamma(3k+6)}, \tag{21}$$

inserting $k = 1$. The separability probability function (Fig. 49) is

$$p_{K=5}^{X-states}(r_A, r_B) = \tag{22}$$

$$\begin{cases} \frac{-21(r_A+5)r_B^6+63(5r_A+1)r_B^4-27r_A(8r_A+5)r_B^2+r_A(8r_A(r_A+2)(r_A+3)+25)-27r_B^2+5}{8\left(-6r_A(r_A+5)r_B^2+r_A(r_A+1)(r_A(r_A+4)+5)+21r_B^4-6r_B^2+1\right)} & r_A > r_B \\ \frac{-21r_A^6(r_B+5)+63r_A^4(5r_B+1)-27r_A^2(r_B(8r_B+5)+1)+25r_B+8r_B^2(r_B+2)(r_B+3)+5}{8\left(-6r_A^2(r_B(r_B+5)+1)+21r_A^4+r_B(r_B+1)(r_B(r_B+4)+5)+1\right)} & r_A < r_B \end{cases}$$

In Fig. 50, we show the $r_A = r_B$ and $r_A = 1 - r_B$ sections of this plot. The minimum of the $r_A = 1 - r_B$ section is once again found at $r = \frac{1}{2}$ with a value of $\frac{1261}{2176} = \frac{13 \cdot 97}{2^7 \cdot 17} \approx 0.579504$ there. For the $r_A = r_B$ section (cf. (12))

$$p_{K=5}^{X-states}(r_A, r_B)(r_A = r_B) = \frac{(1-r)(r(21r(r(r+8)+6)+40)+5)}{8(r(16r+7)+1)}. \tag{23}$$

The maximum of 0.63964 of this curve is attained at $r = 0.238465$.

D. Random Induced $K = 6$ case

Here the total volume itself is $\frac{\pi^2}{9081072000} \approx 1.0868325 \cdot 10^{-9}$. The marginal distributions are of the form

$$V_{K=6}^{(X)}(r) = \frac{\pi^2 \left(1-r^2\right)^7}{2890137620} = \frac{\pi^2 \left(1-r^2\right)^7}{2^{18} \cdot 3^2 \cdot 5^2 \cdot 7^2}. \tag{24}$$

The separability probability is $\frac{26}{33}$, given by (21), inserting $k = 2$.

E. Random Induced $K = 7$ case

Here the total volume itself is $\frac{\pi^2}{5866372512000} \approx 1.68240328 \cdot 10^{-12}$. The marginal distributions are of the form

$$V_{K=7}^{(X)}(r) = \frac{\pi^2 \left(r^2-1\right)^9}{1664719257600} = \frac{\pi^2 \left(r^2-1\right)^9}{2^{24} \cdot 3^4 \cdot 5^2 \cdot 7^2}. \tag{25}$$

The separability probability is $\frac{125}{143}$, given by (21), inserting $k = 3$.

F. Random Induced $K = 3$ case

The total volume is $\frac{2}{3}\pi^2 \log^2(2) \approx 3.16125412$. The bivariate total volume distribution is

$$ {}_{tot}V^{(X)}_{K=3}(r_A, r_B) = \begin{cases} -2\pi^2 \log^2(2)\,(r_A - 1) & r_A > r_B \wedge r_A + r_B > 0 \wedge r_A < 1 \\ -2\pi^2 \log^2(2)\,(r_B - 1) & r_B > r_A \wedge r_A + r_B > 0 \wedge r_B < 1 \end{cases} \tag{26} $$

The two marginal distributions are of the form $\pi^2\,(1 - r^2) \log^2(2)$. Here we found the separability probability to equal $\frac{1}{3}$. We have not been able to find analytic formulas for the bivariate separability volume function and the bivariate separability probability function, but in Fig. 51, we present a numerically-based estimate of the separability probability function.

X. APPENDIX B: SEPARABILITY PROBABILITIES AS A FUNCTION OF $||\rho - \rho^A \otimes \rho^B||_{HS}$

In a recent paper of Holik and Plastino, the expression

$$ ||\rho - \rho^A \otimes \rho^B||_{HS} \tag{27} $$

is put forth as a measure of entanglement [29, eq. (9)], where $||\ldots||_{HS}$ is the Hilbert-Schmidt norm

$$ ||A||^2_{HS} = \mathrm{tr}(AA^\dagger). \tag{28} $$

In Fig. 52 we show estimates of the two-qubit separability probabilities as a function of this term for the Hilbert-Schmidt and Bures measures, based on 54,000,000 random realizations in the former case and 43,000,000 in the latter (cf. [6, Fig. 2]). The probability diminishes as the Hilbert-Schmidt distance from product states ($\rho^A \otimes \rho^B$) increases. (Of course, it might be of some interest to employ Bures counterparts of (27) and (28)).

---

[1] P. B. Slater, J. Phys. A **40**, 14279 (2007).

[2] P. B. Slater and C. F. Dunkl, J. Phys. A **45**, 095305 (2012).

[3] P. B. Slater, J. Phys. A **46**, 445302 (2013).

[4] J. Fei and R. Joynt, arXiv.1409:1993.

[5] P. B. Slater and C. F. Dunkl, J. Geom. Phys. **90**, 42 (2015).

[6] A. Khvedelidze and I. Rogojin, Zap. Nauchn. Sem. POMI **432**, 274 (2015).

[7] K. M. Fonseca-Romero, J. M. Martinez-Rincón, and C. Viviescas, Phys. Rev. A **86**, 042325 (2012).

[8] J. Shang, Y.-L. Seah, H. K.Ng, D. J. Nott, and B.-T. Englert, New J. Phys. **17**, 043017 (2015).

[9] K. Życzkowski and H.-J. Sommers, J. Phys. A **36**, 10115 (2003).

[10] I. Bengtsson and K. Życzkowski, *Geometry of Quantum States* (Cambridge, Cambridge, 2006).

[11] S. Milz and W. T. Strunz, J. Phys. A **48**, 035306 (2015).

[12] S. Jevtic, M. Pusey, D. Jennings, and T. Rudolph, Phys. Rev. Lett. **113**, 020402 (2014).

[13] K. Życzkowski and H.-J. Sommers, J. Phys. A **A34**, 7111 (2001).

[14] G. Aubrun, S. J. Szarek, and D. Ye, Commun. Pure Appl. Math. **LXVII**, 0129 (2014).

[15] P. B. Slater and C. F. Dunkl, Adv. Math. Phys. **2015**, 621353 (2015).

[16] F. J. Bloore, J. Phys. A **9**, 2059 (1976).

[17] P. B. Slater, Phys. Rev. A **75**, 032326 (2007).

[18] P. B. Slater, J. Geom. Phys. **58**, 1101 (2008).

[19] P. B. Slater, J. Phys. A **42**, 465305 (2009).

[20] R. Hildebrand, J. Math. Phys. **48**, 102108 (2007).

[21] K. Życzkowski, P. Horodecki, A. Sanpera, and M. Lewenstein, Phys. Rev. A **58**, 883 (1998).

[22] R. Mosseri and R. Dandoloff, J. Phys. A **34**, 10243 (2001).

[23] R. Mosseri and P. Ribeiro, Math. Structures in Comp. Sci. **17**, 1117 (2007).

[24] H.-J. Sommers and K. Życzkowski, J. Phys. A **36**, 10083 (2003).

[25] P. J. Forrester and M. Kieburg, arXiv:1410.6883.

[26] C. M. Caves, C. A. Fuchs, and P. Rungta, Found. Phys. Letts. **14**, 199 (2001).

[27] J. Batle, A. R. Plastino, M. Casas, and A. Plastino, Opt. Spect. **94**, 759 (2003).

[28] P. B. Slater, arXiv:1504.04555.

[29] F. Holik and A. Plastino, Phys. Rev. A **84**, 062327 (2011).

[30] P. Mendonça, M. A. Marchiolli, and D. Galetti, Anns. Phys. **351**, 79 (2014).

[31] N. Balakrishnan and C. Lai, *Continuous Bivariate Distributions* (Springer, New York, 2009).

[32] V. A. Osipov, H.-J. Sommers, and K. Życzkowski, J. Phys. A **43**, 055302 (2010).

[33] M. Demianowicz, Phys. Rev. A **83**, 034301 (2011).

[34] A. Peres, Phys. Rev. Lett. **77**, 1413 (1996).

[35] M. Horodecki, P. Horodecki, and R. Horodecki, Phys. Lett. A **223**, 1 (1996).

[36] E. A. Sungur and P. Ng, Commun. Stat.–Theory and Methods **34**, 2269 (2005).

[37] H. Braga, S. Souza, and S. S. Mizrahi, Phys. Rev. A **81**, 042310 (2010).

[38] V. E. Mkrtchian and V. O. Chaltykyan, Opt. Commun. **63**, 239 (1987).

[39] J. A. Miszczak, Comput. Phys. Commun. **183**, 118 (2012).

[40] J. A. Miszczak, Comput. Phys. Commun. **184**, 257 (2013).

[41] P. B. Slater, Euro. Phys. J. B **17**, 471 (2000).

[42] P. B. Slater, J. Geom. Phys. **53**, 74 (2005).

[43] I. Dumitriu, A. Edelman, and G. Shuman, J. Symb. Comp **42**, 587 (2007).

[44] R. B. Nelsen, *An Introduction to Copulas* (Springer-Verlag, New York, 1998).

[45] P. Kumar, Appl. Math. Sci. **4**, 657 (2010).

[46] S. Guillotte and F. Perron, Bernouilli **18**, 496 (2012).

[47] I. Kojadinovic and J. Yan, Stat. Comput. **21**, 17 (2011).

[48] L. Ruschendorf, B. Schweizer, and M. D. Taylor, *Distributions with fixed marginals and related topics* (Institute of Mathematical Statistics, Hayward, CA, 1996).

[49] D. C. Brody and E.-M. Graefe, Phys. Rev. D **84**, 125016 (2011).

[50] I. Dumitriu and A. Edelman, J. Math. Phys. **43**, 5830 (2002).

[51] H. Scutaru, Proc. Romanian Acad., Ser. A **5**, 1 (2004).

[52] U. Fano, Rev. Mod. Phys. **55**, 855 (1983).

[53] C. F. Dunkl and P. B. Slater, arXiv:1501.02289 (to appear in Random Matrices: Theory and Applications).

Acknowledgments

I would like to express appreciation to the Kavli Institute for Theoretical Physics (KITP) for computational support in this research, as well as Simon Milz and Charles Dunkl–who suggested the use of confidence bands–for helpful communications.

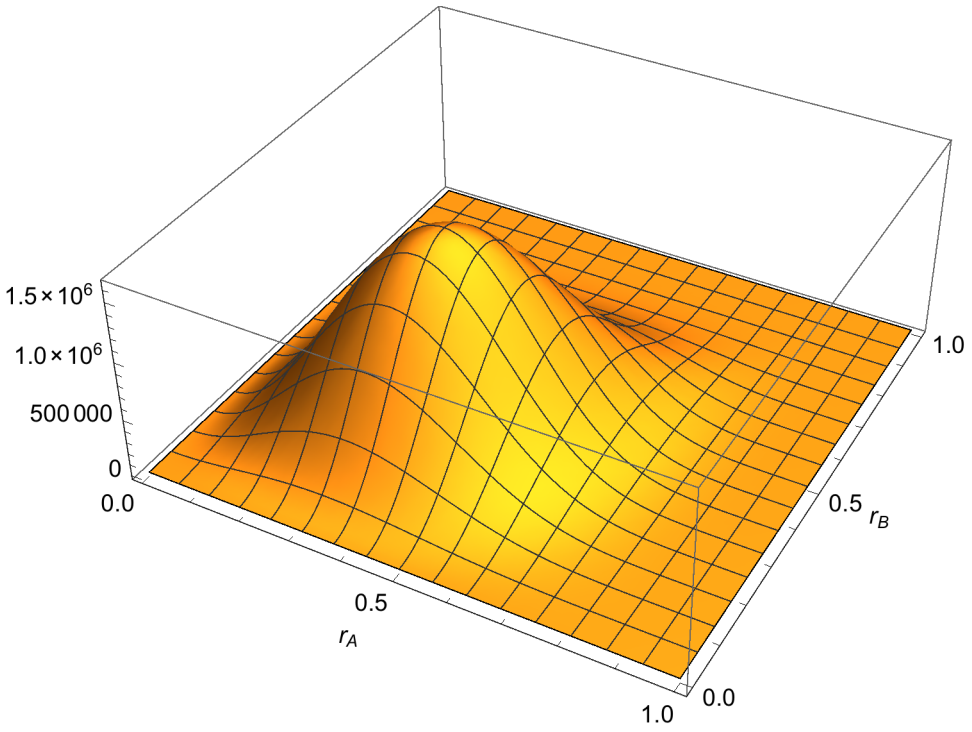


FIG. 1: Histogram of Hilbert-Schmidt randomly sampled two-qubit density matrices parameterized by r_A and r_B

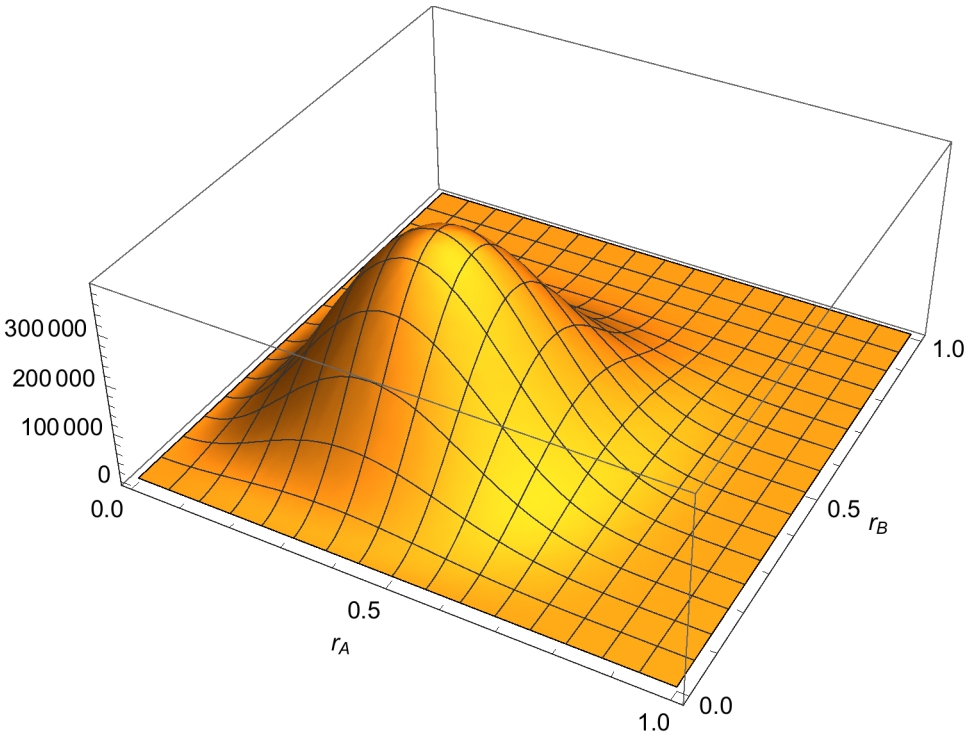


FIG. 2: Histogram of Hilbert-Schmidt randomly sampled *separable* two-qubit density matrices parameterized by r_A and r_B

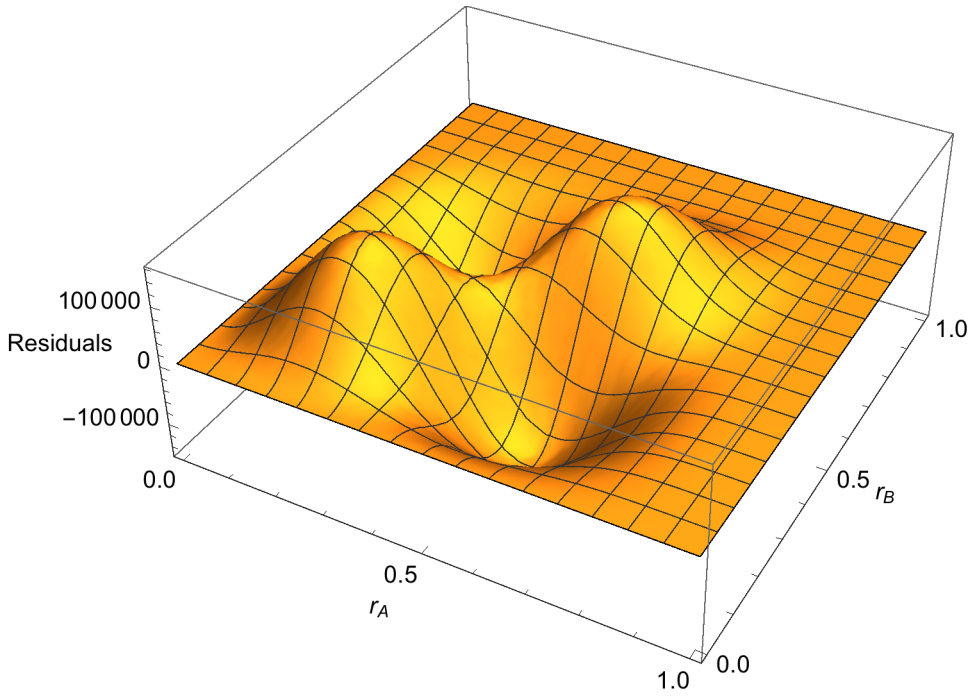


FIG. 3: Residuals from a fit to the total counts (Fig. 1) of a normalized form of $16\pi^2 r_A^2 r_B^2 (1-r_A^2)^6 (1-r_B^2)^6$

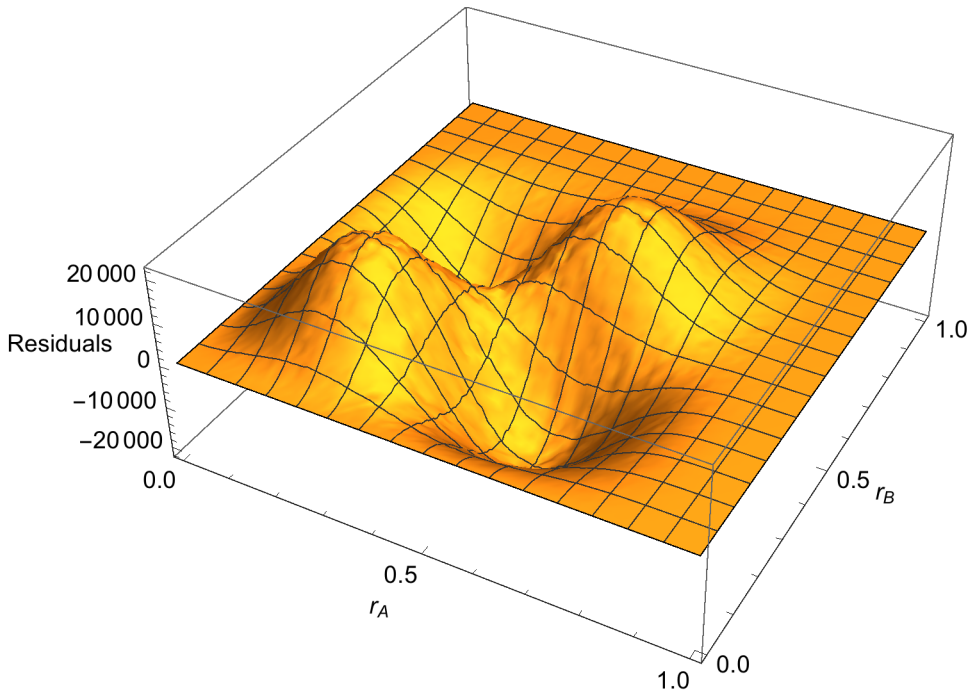


FIG. 4: Residuals from a fit to the separable counts (Fig. 2) of a normalized form of $16\pi^2 r_A^2 r_B^2 (1-r_A^2)^6 (1-r_B^2)^6$

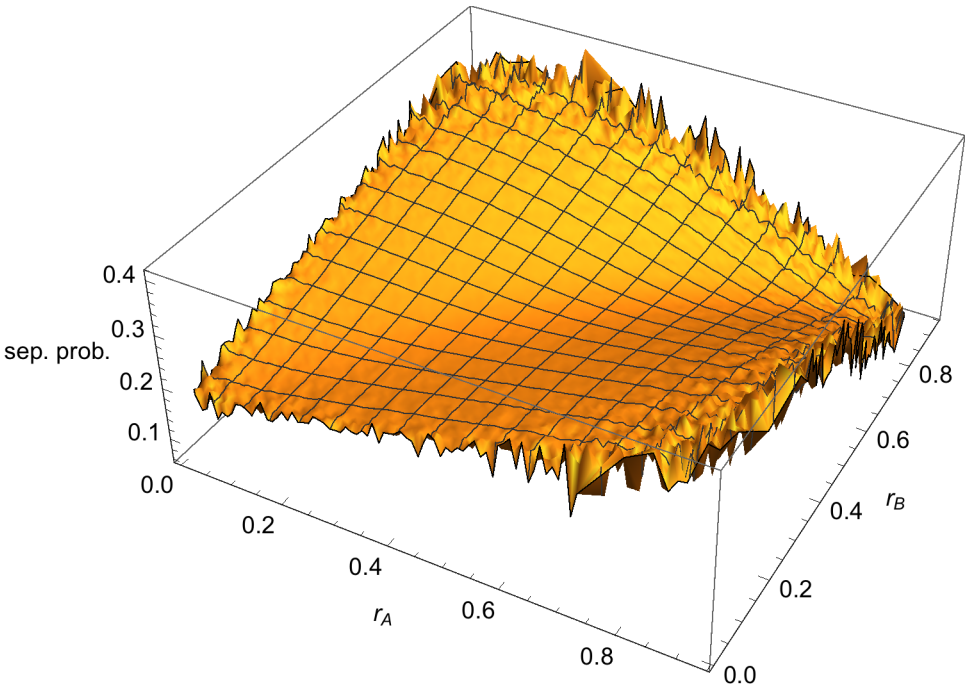


FIG. 5: Estimated joint Hilbert-Schmidt two-qubit separability probabilities

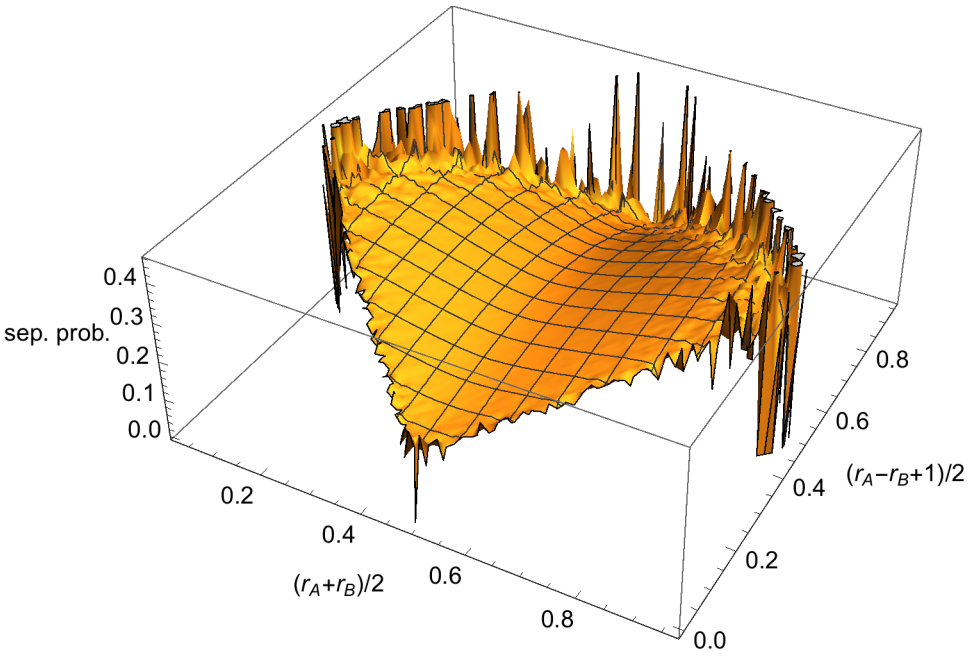


FIG. 6: $\frac{\pi}{4}$-rotation of estimated joint Hilbert-Schmidt two-qubit separability probabilities (Fig. 5)

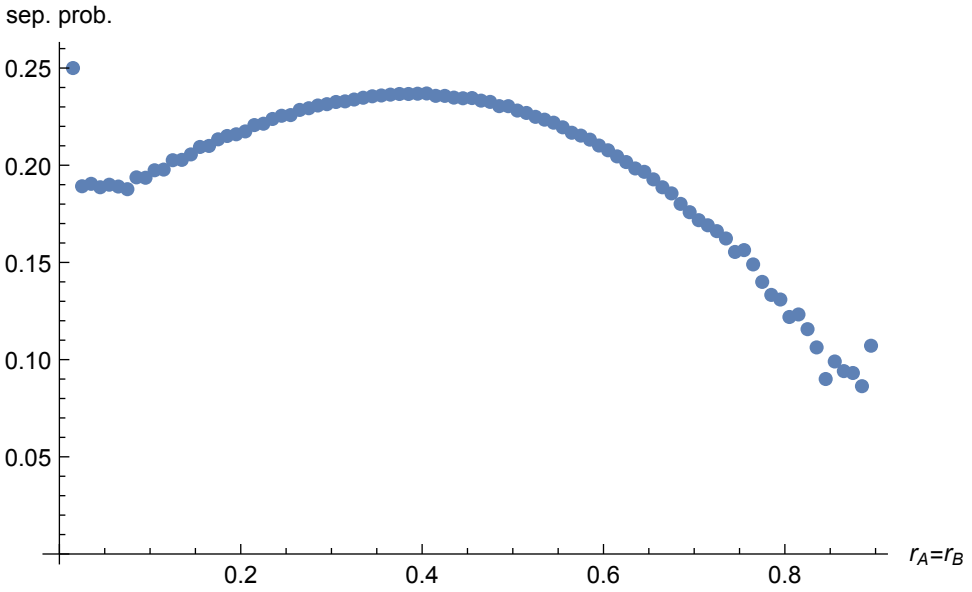


FIG. 7: Estimated Hilbert-Schmidt separability probabilities for $r_A = r_B$. A closely-fitting model (ratio of apparent separable and total volumes) for this curve is $\frac{375(1-r)\left(58r^2+17r+2\right)}{4096(8r+1)}$.

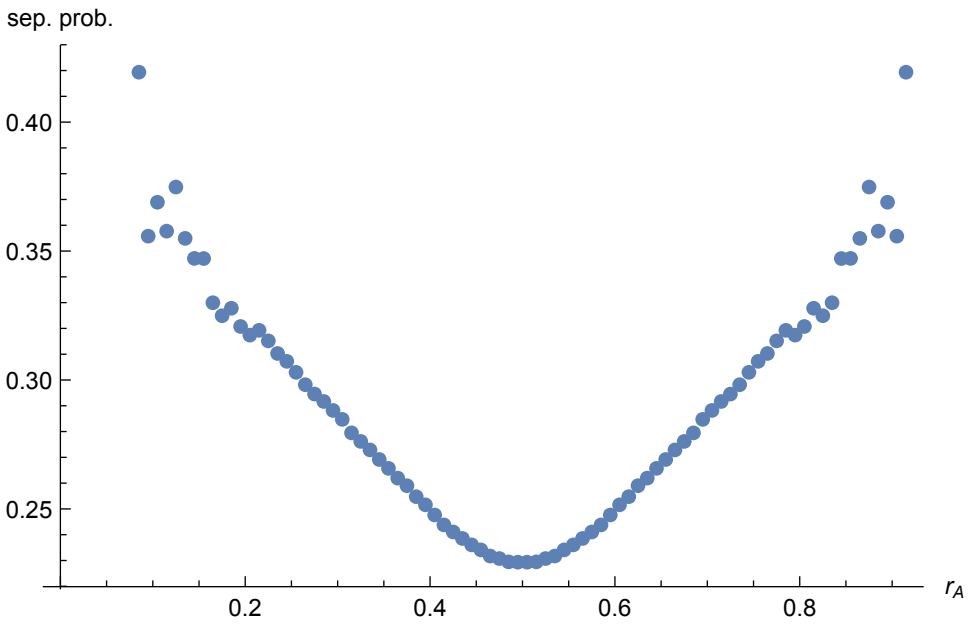


FIG. 8: Estimated Hilbert-Schmidt two-qubit separability probabilities for $r_A + r_B = 1$. A closely-fitting model for this curve is $\frac{r+4}{24r+8}$ $(0 < r < \frac{1}{2})$ and $\frac{r-5}{24r-32}$ $(\frac{1}{2} < r < 1)$.

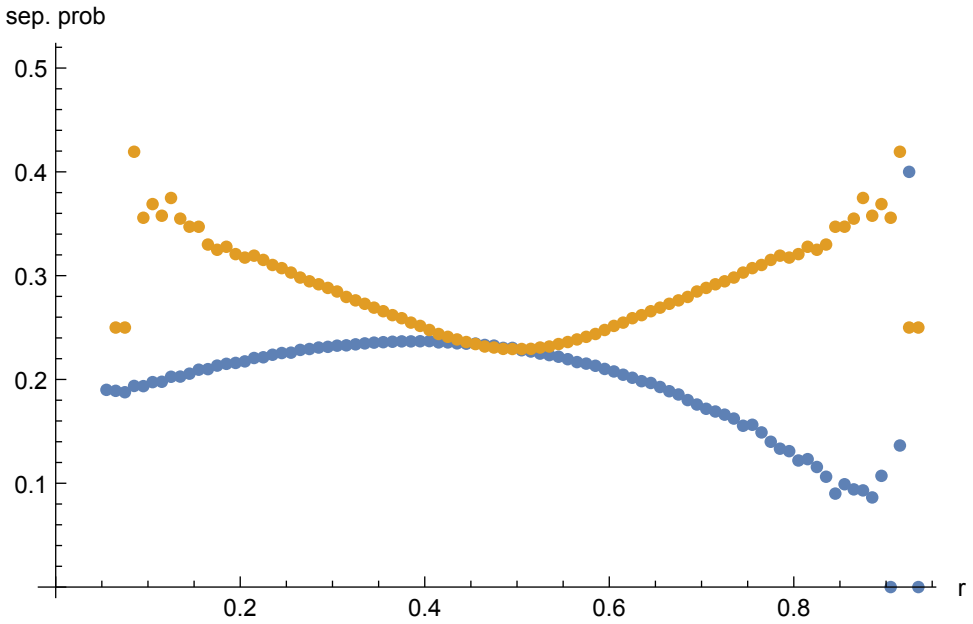


FIG. 9: Joint plot of last two figures

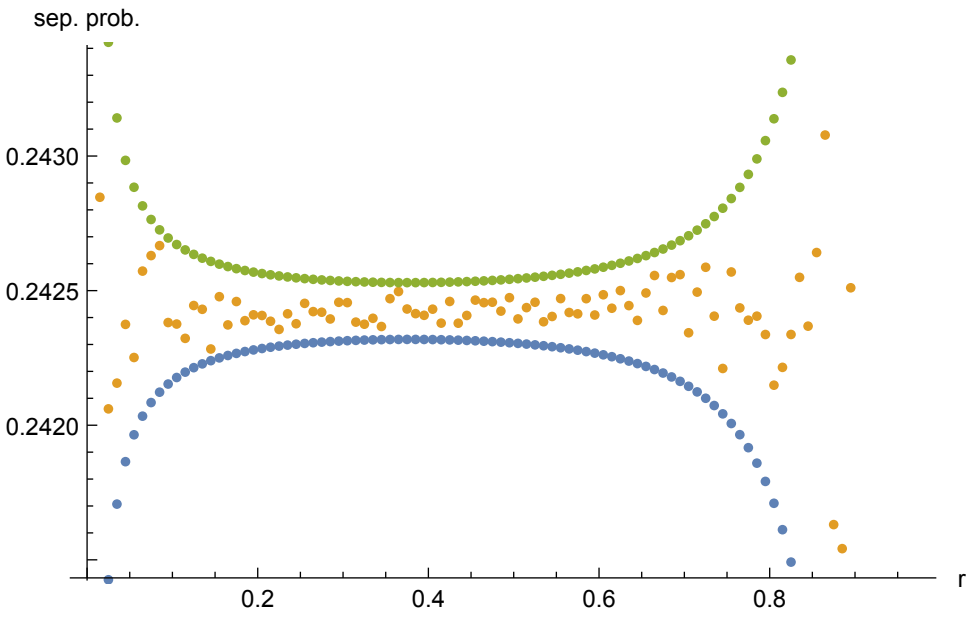


FIG. 10: Estimated (marginal) Hilbert-Schmidt two-qubit separability probabilities along either Bloch radius, together with 95% confidence limits about the conjectured value of $\frac{8}{33} \approx 0.242424$

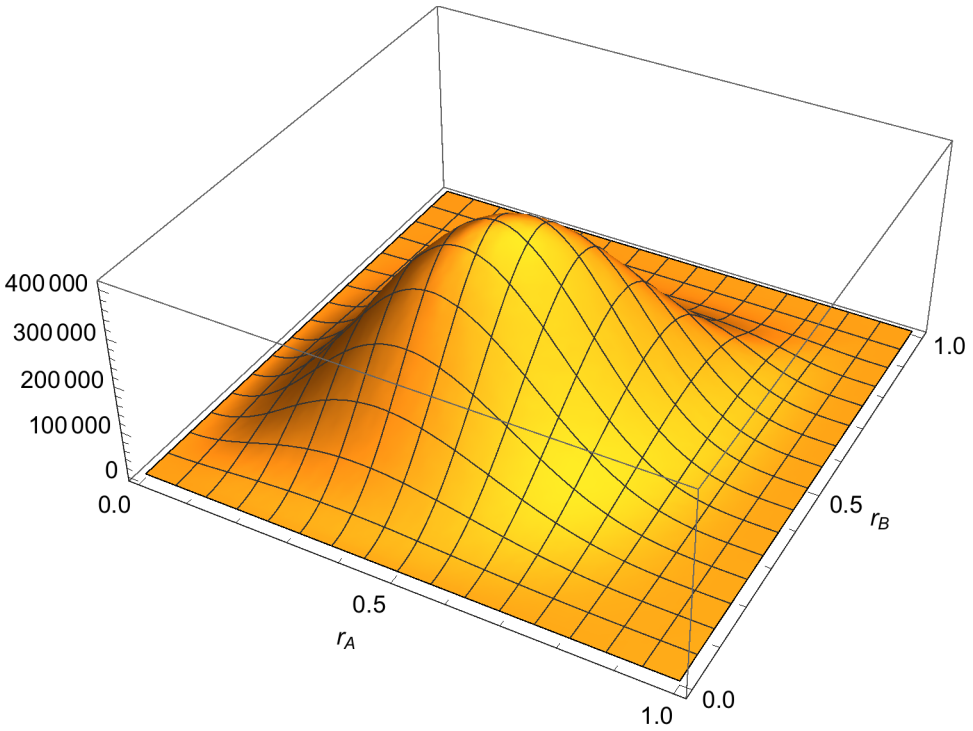


FIG. 11: Histogram of randomly sampled (with respect to the random induced $K = 3$ measure) two-qubit density matrices

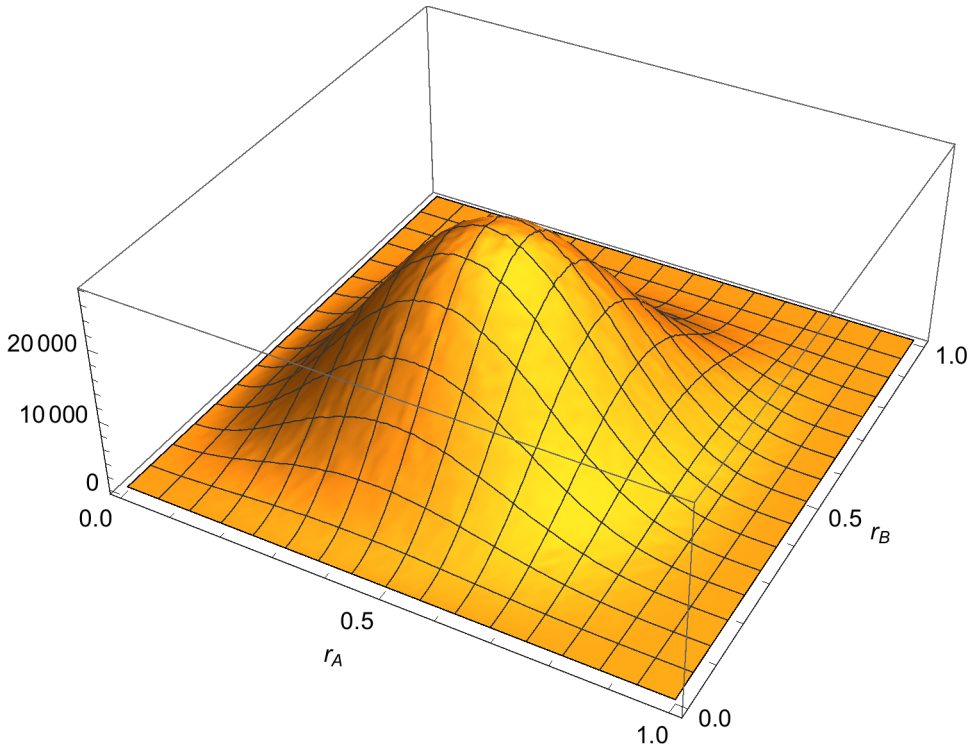


FIG. 12: Histogram of randomly sampled (with respect to the random induced $K = 3$ measure) *separable* two-qubit density matrices

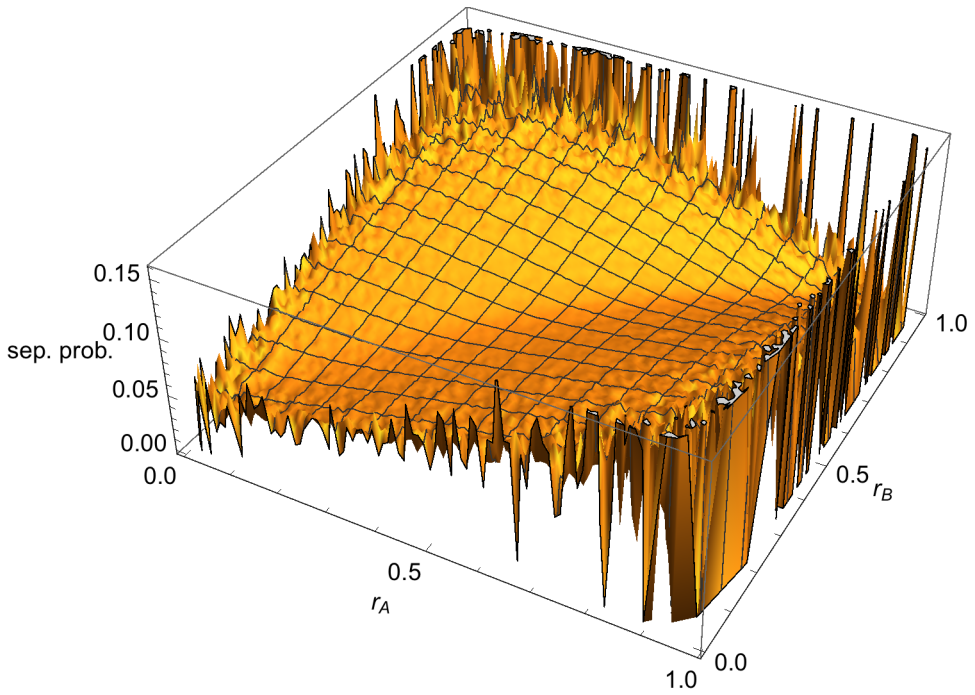


FIG. 13: Estimated joint random induced ($K = 3$) separability probabilities

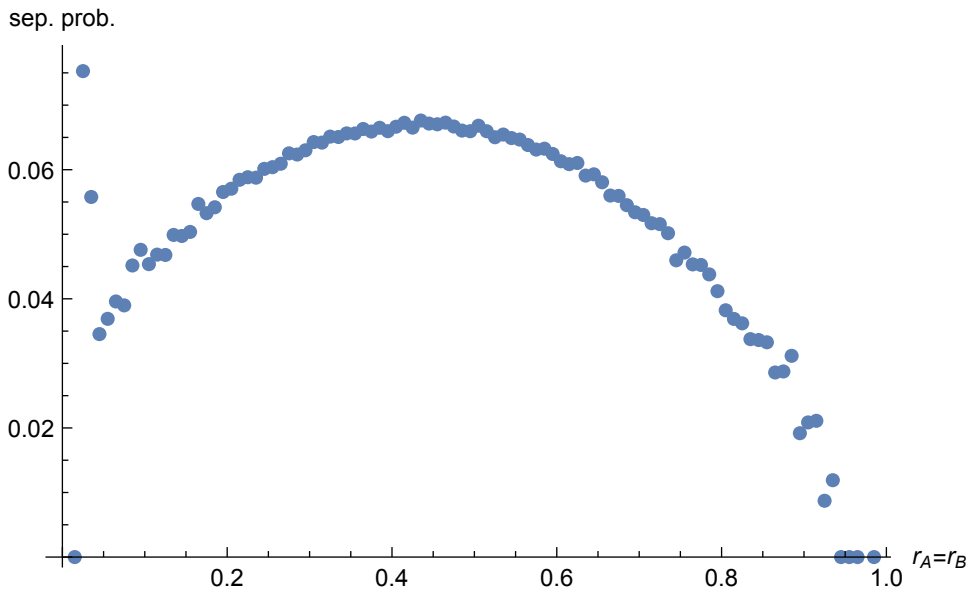


FIG. 14: Estimated random induced ($K = 3$) two-qubit separability probabilities for $r_A = r_B$. A closely-fitting model (ratio of apparent separable and total volumes) for this curve is $\frac{1}{32}(1-r)\,(r^2+6r+1)$, giving a total separability probability for the continuum of such states of $\frac{9}{143} \approx 0.0629371$. The maximum of the curve $\frac{1}{27}(5\sqrt{10}-14) \approx 0.0670885$ occurs at $r = \frac{1}{3}(2\sqrt{10}-5) \approx 0.441518$

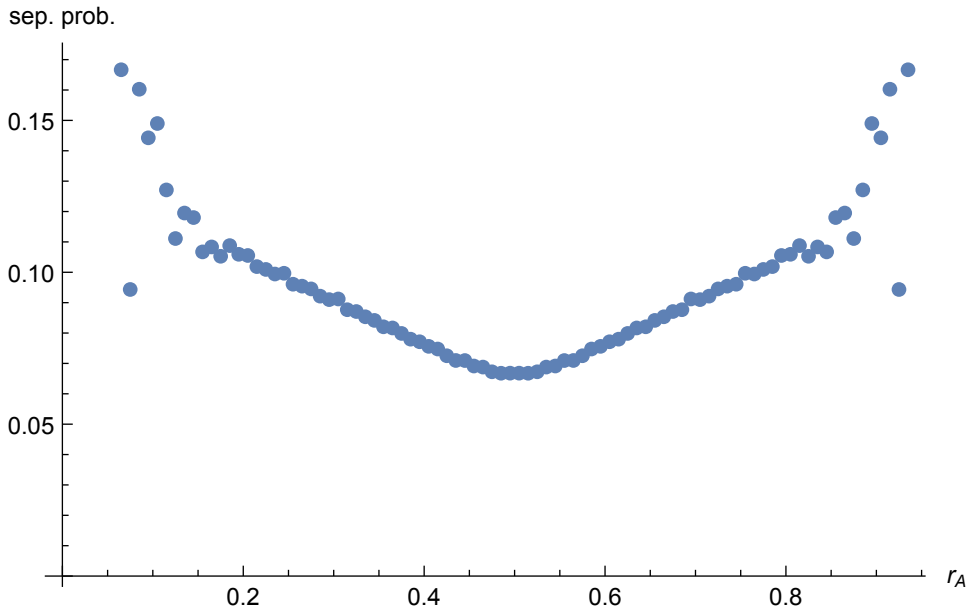


FIG. 15: Estimated random induced ($K = 3$) two-qubit separability probabilities for $r_A + r_B = 1$. A closely-fitting model for this curve is $\frac{1-r}{8}$ $(0 < r < \frac{1}{2})$ and $\frac{r}{8}$ $(\frac{1}{2} < r < 1)$, with the minimum of $\frac{1}{16}$ occurring at $r = \frac{1}{2}$.

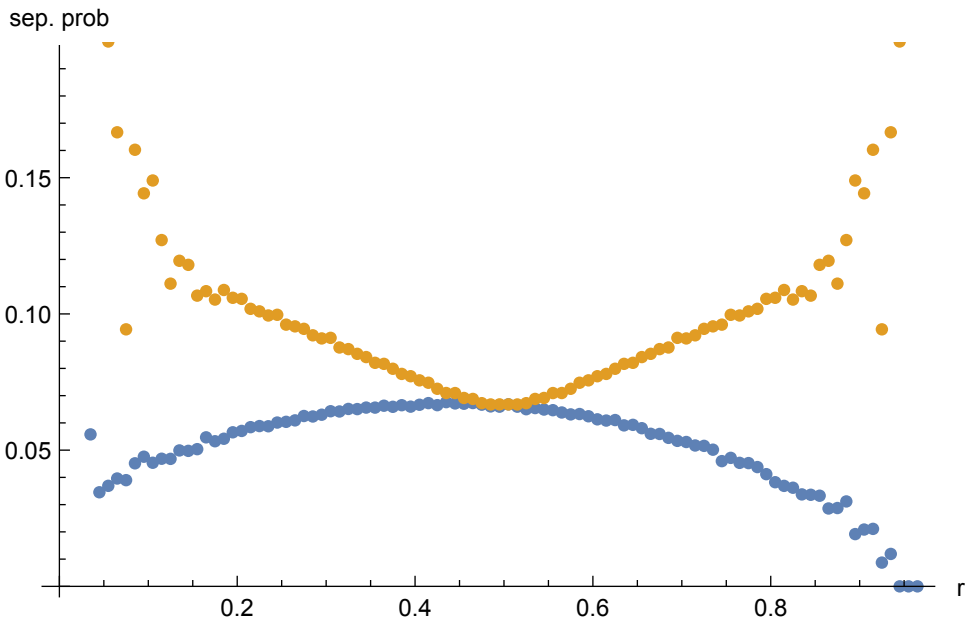


FIG. 16: Joint plot of last two figures

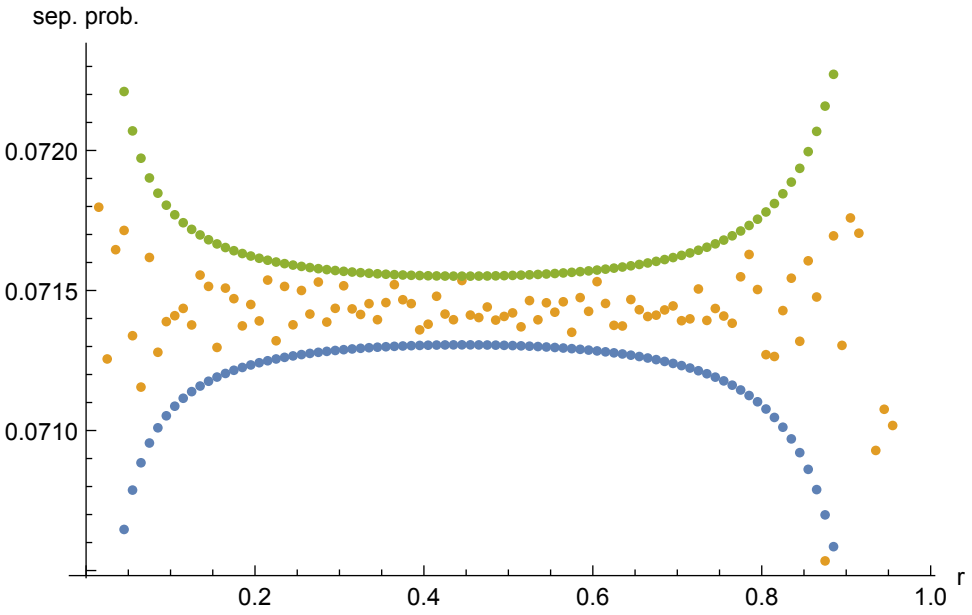


FIG. 17: Estimated random induced ($K = 3$) two-qubit separability probabilities over either one of the Bloch radii, along with 95% confidence limits about the conjectured value of $\frac{1}{14} \approx 0.0714285$

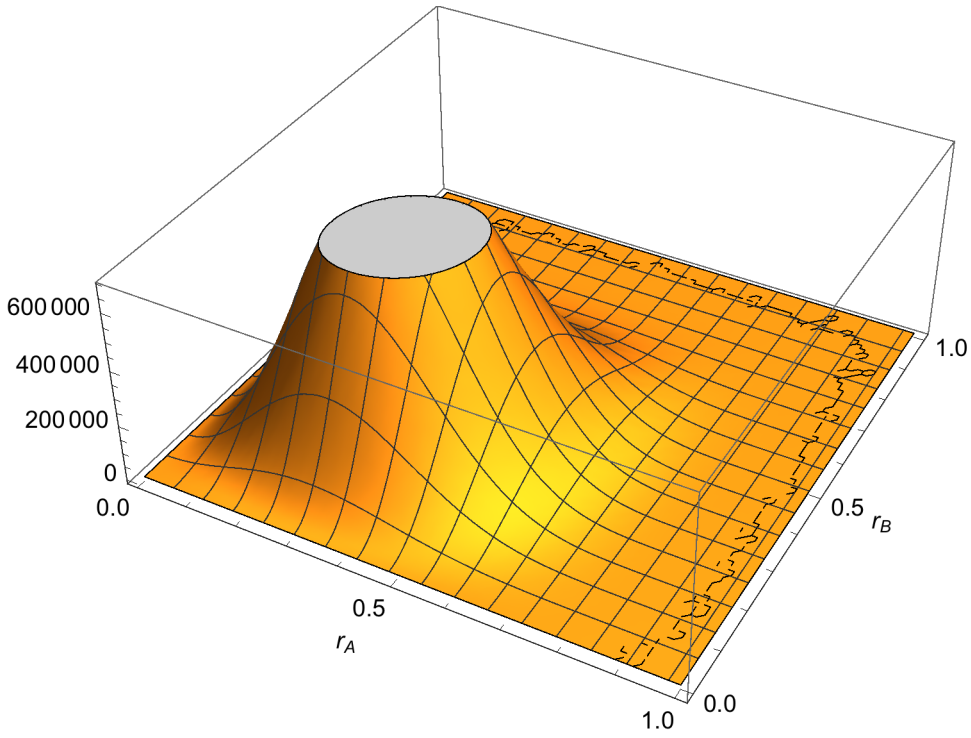


FIG. 18: Histogram of randomly sampled (with respect to the random induced $K = 5$ measure) two-qubit density matrices

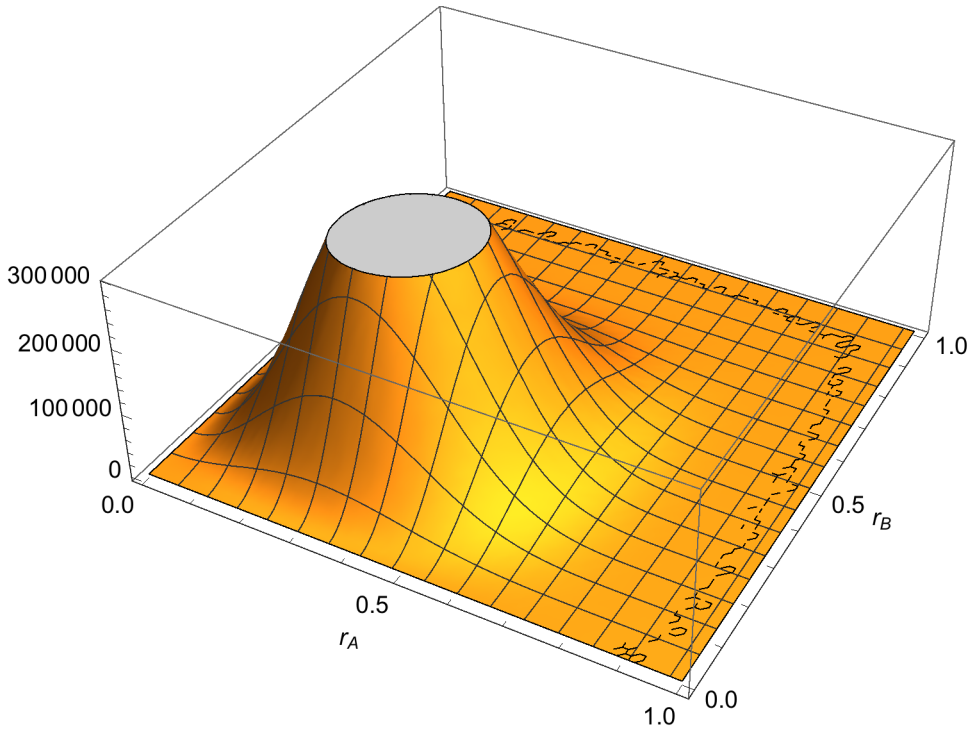


FIG. 19: Histogram of randomly sampled (with respect to the random induced $K = 5$ measure) *separable* two-qubit density matrices

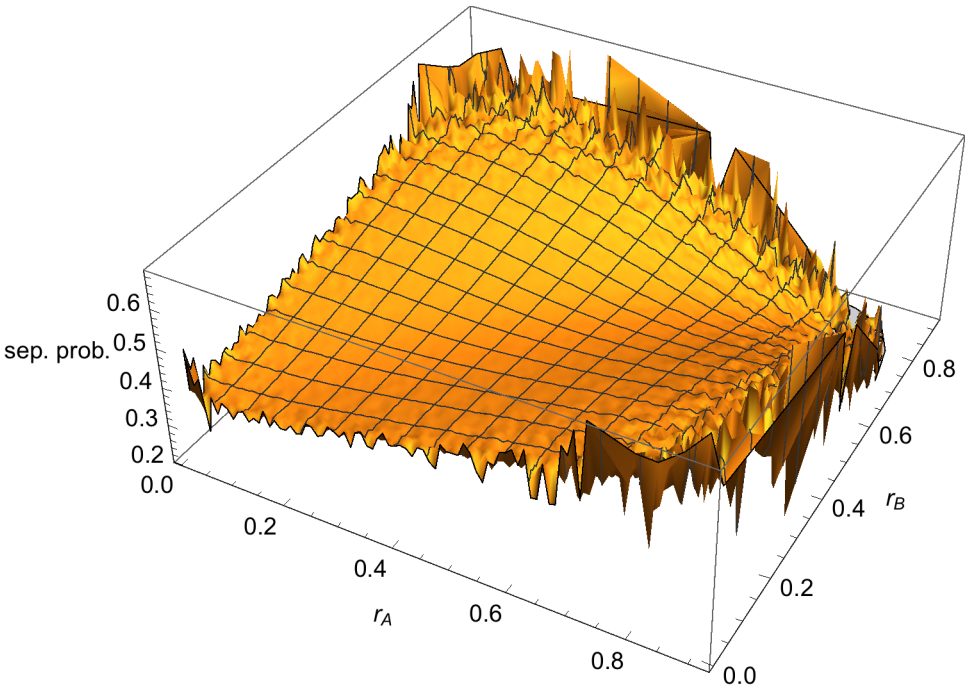


FIG. 20: Estimated joint random induced ($K = 5$) separability probabilities

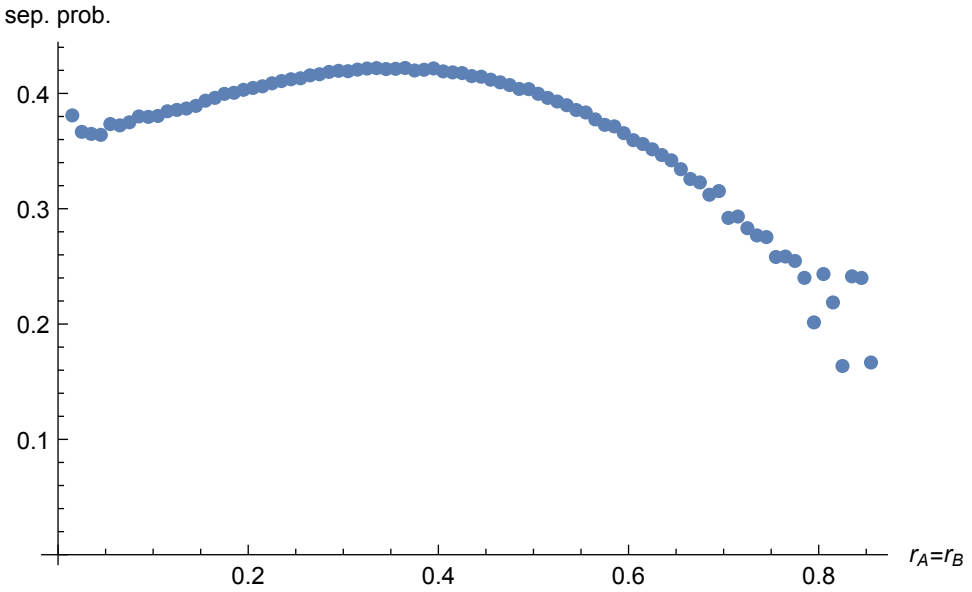


FIG. 21: Estimated random induced ($K = 5$) two-qubit separability probabilities for $r_A = r_B$. A closely-fitting model (ratio of apparent separable and total volumes) for this curve is $\frac{(1-r)\left(\frac{87r^3}{2}+\frac{85r^2}{4}+\frac{17r}{4}+\frac{1}{3}\right)}{40r^2+11r+1}$.

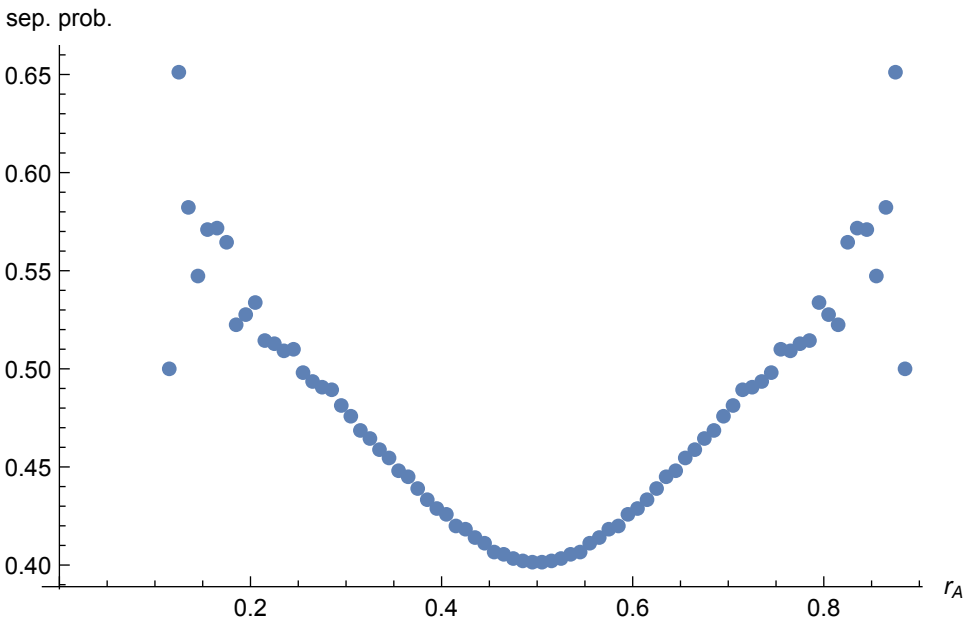


FIG. 22: Estimated random induced ($K = 5$) two-qubit separability probabilities for $r_A + r_B = 1$.

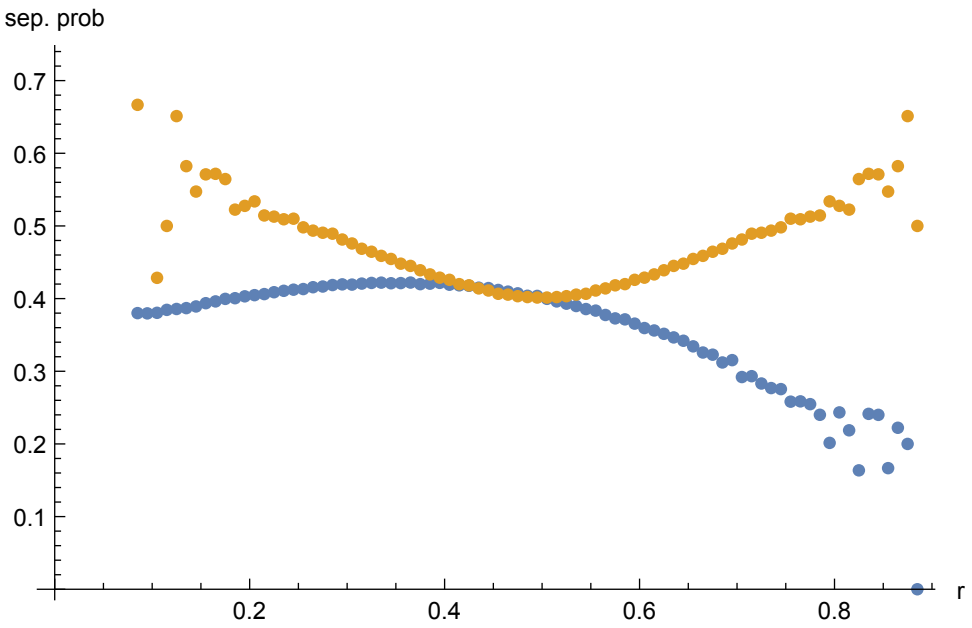


FIG. 23: Joint plot of last two figures

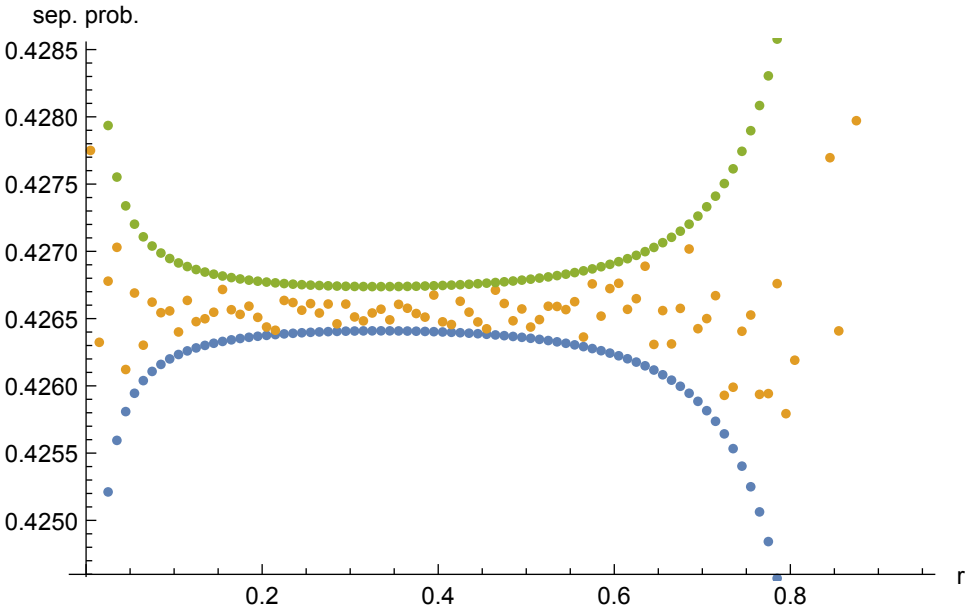


FIG. 24: Estimated random induced ($K = 5$) two-qubit separability probabilities over either one of the Bloch radii, along with 95% confidence limits about the conjectured value of $\frac{61}{143} \approx 0.426573$

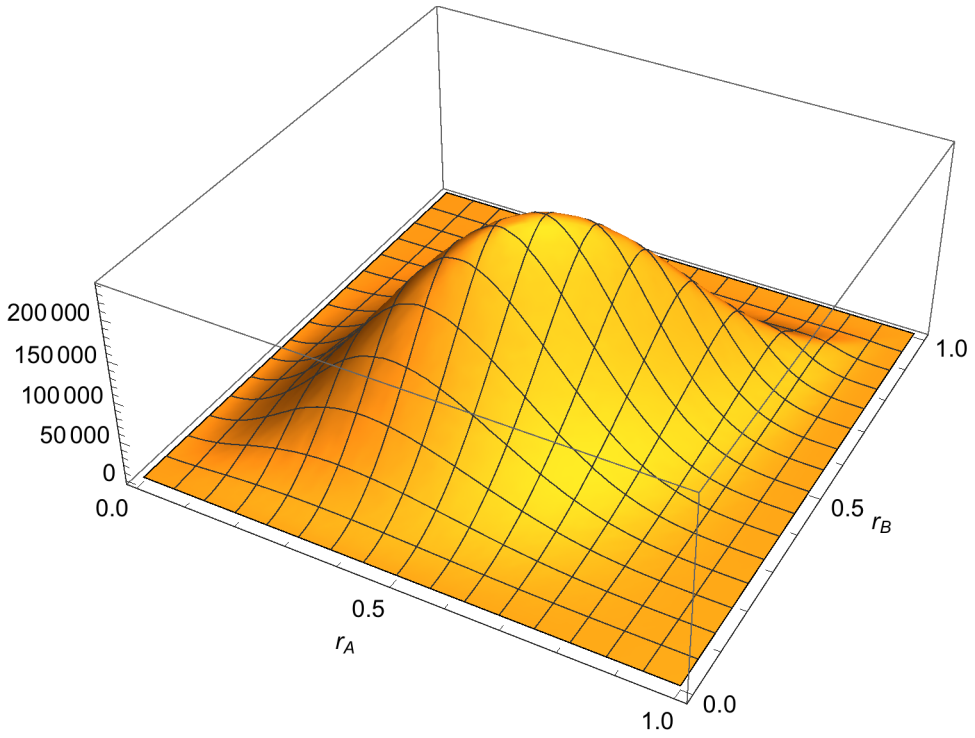


FIG. 25: Histogram of randomly sampled (with respect to the Bures measure) two-qubit density matrices

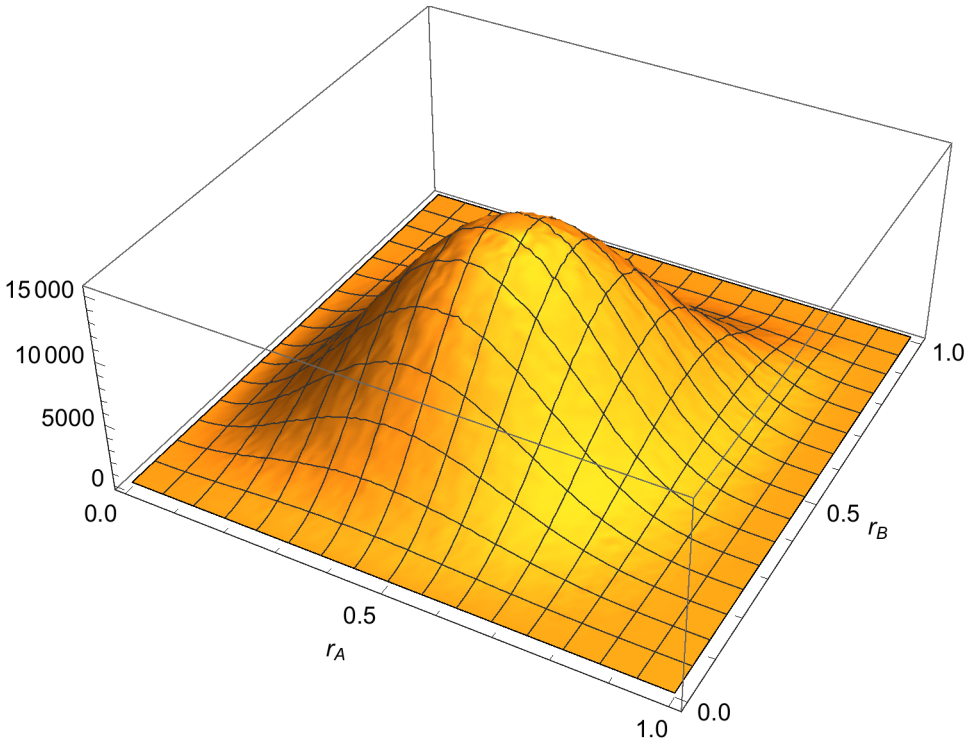


FIG. 26: Histogram of randomly sampled (with respect to the Bures measure) *separable* two-qubit density matrices

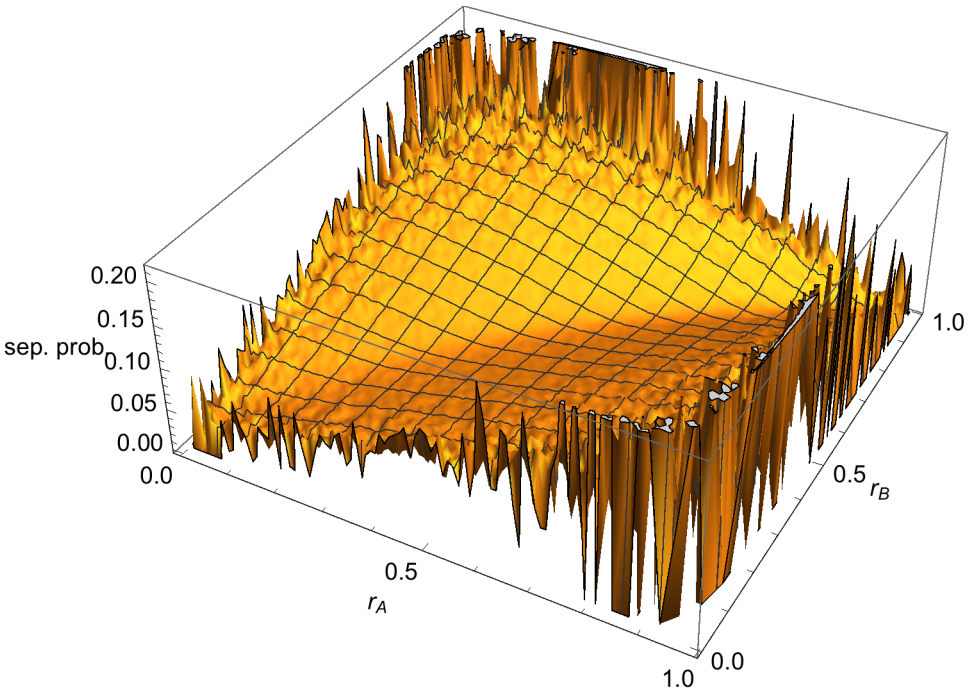


FIG. 27: Estimated joint Bures two-qubit separability probabilities

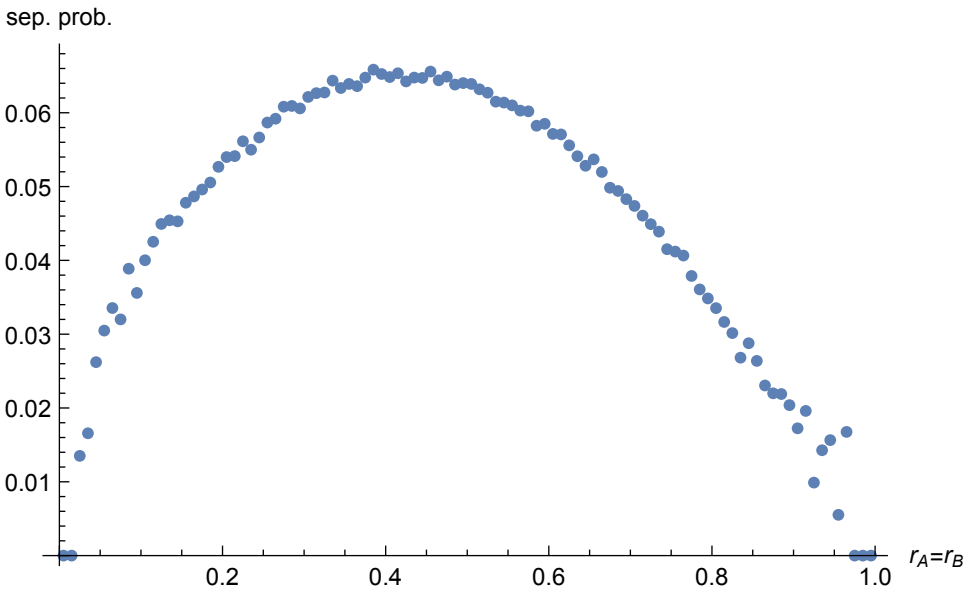


FIG. 28: Estimated Bures two-qubit separability probabilities for $r_A = r_B$

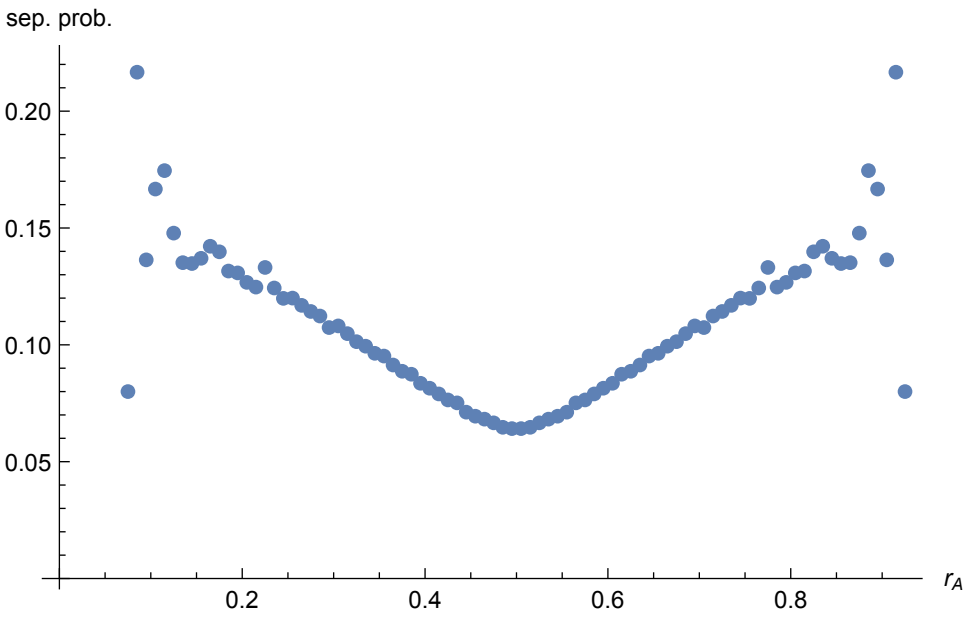


FIG. 29: Estimated Bures two-qubit separability probabilities for $r_A + r_B = 1$

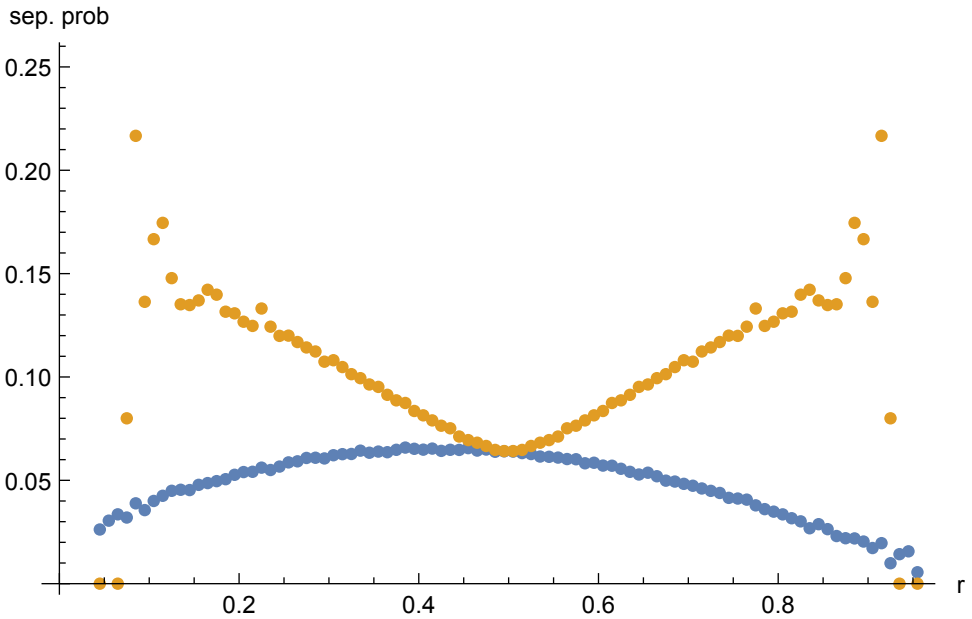


FIG. 30: Joint plot of last two figures

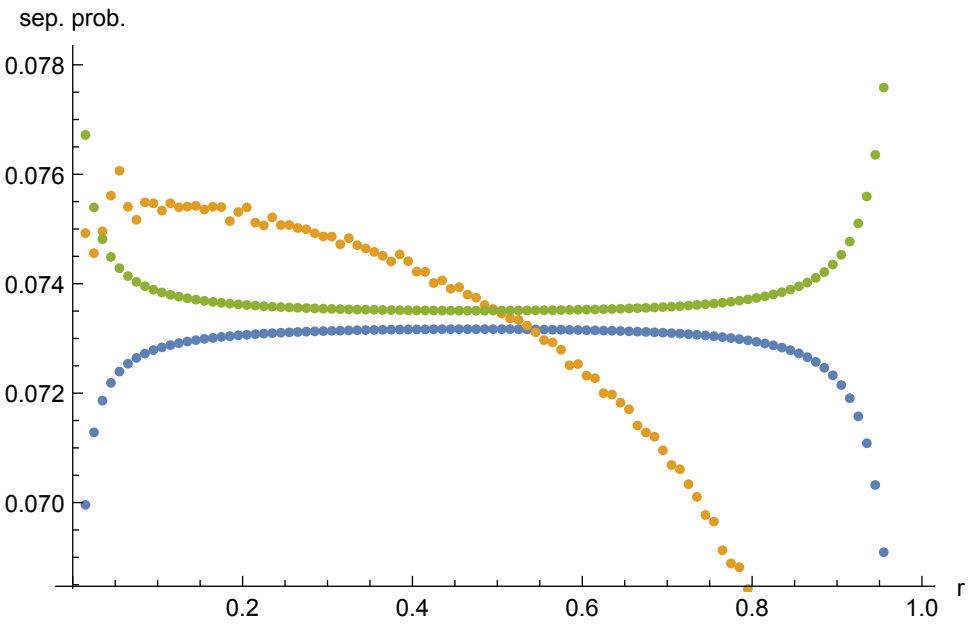


FIG. 31: Estimated Bures two-qubit separability probabilities over either one of the Bloch radii, along with ill-fitting (in contrast to Hilbert-Schmidt and random induced) 95% confidence limits about the conjectured overall probability of $\frac{1680(\sqrt{2}-1)}{\pi^8} \approx 0.0733389$.

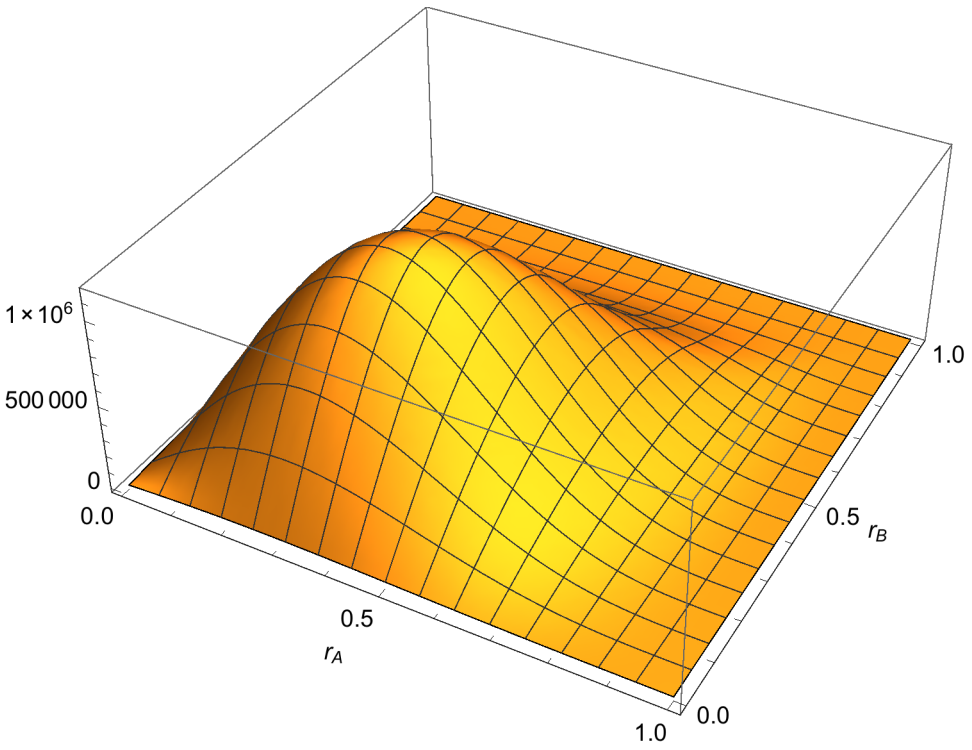


FIG. 32: Histogram of randomly sampled two-*rebit* density matrices

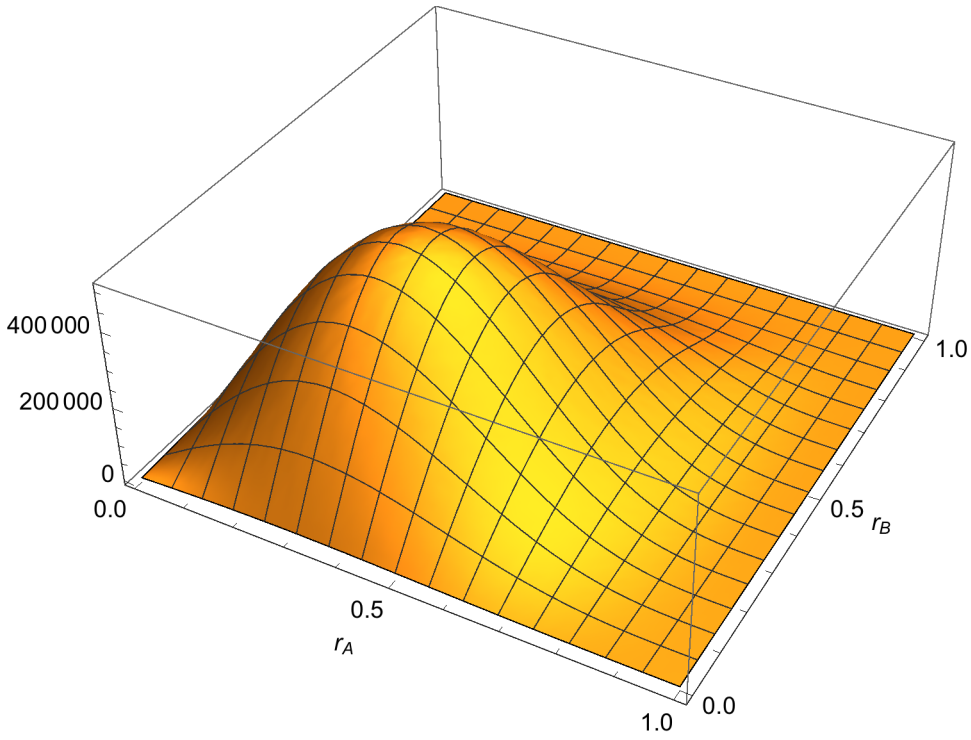


FIG. 33: Histogram of randomly sampled *separable* two-rebit density matrices

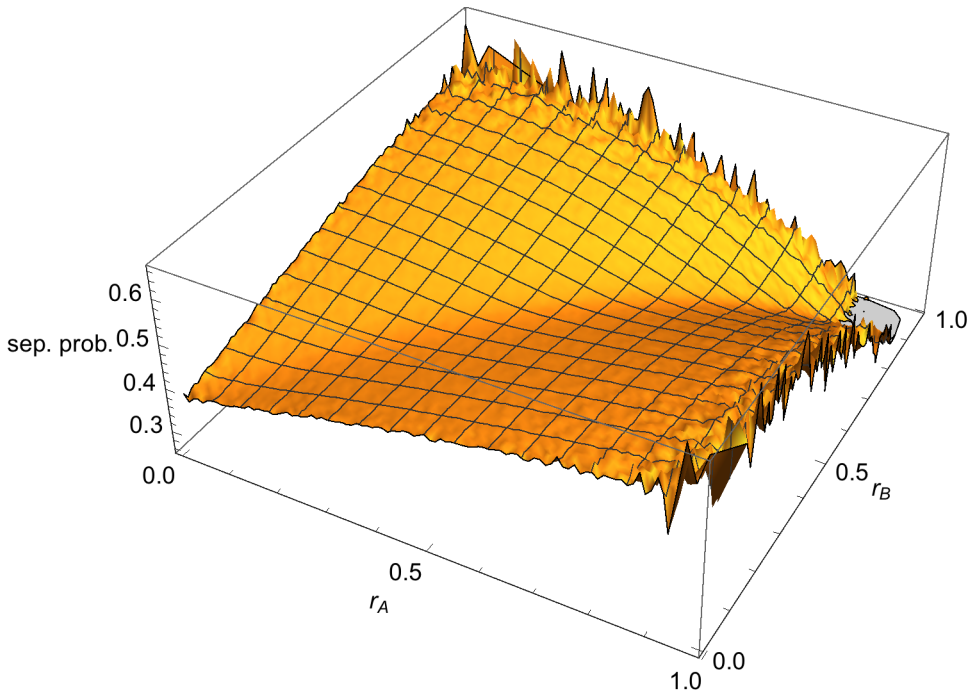


FIG. 34: Estimated joint Hilbert-Schmidt two-*rebit* separability probabilities

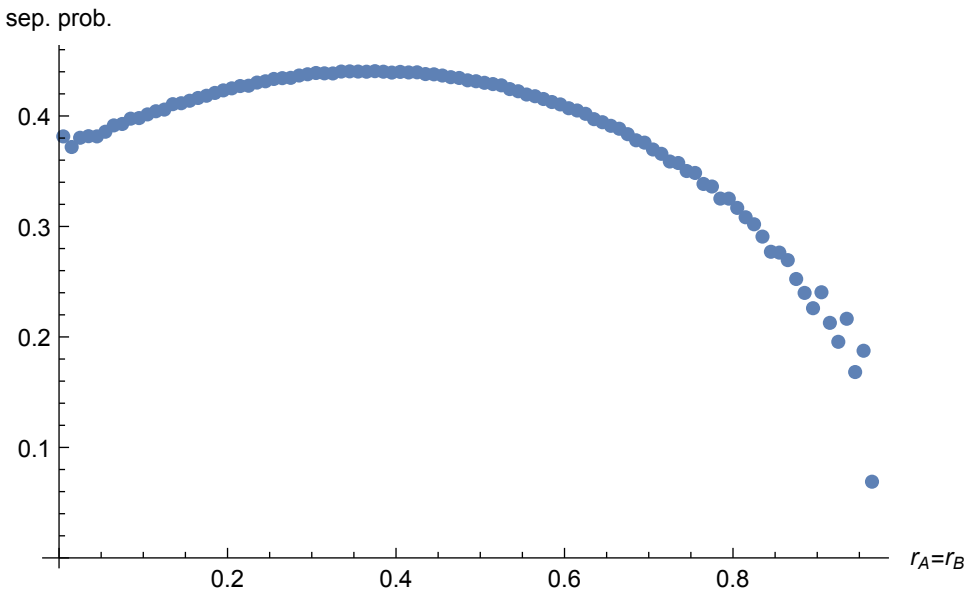


FIG. 35: Estimated Hilbert-Schmidt two-*rebit* separability probabilities for $r_A = r_B$

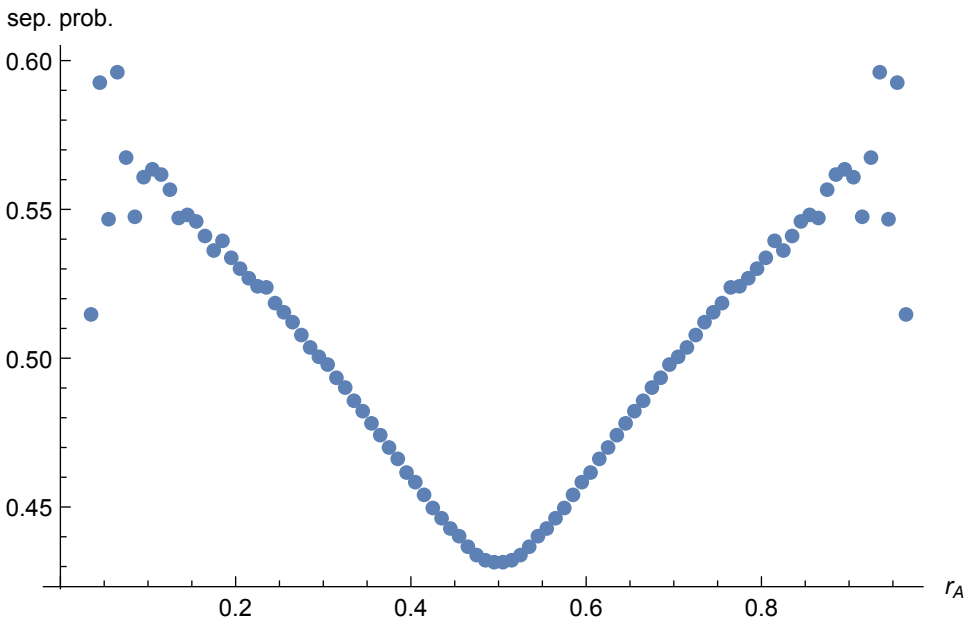


FIG. 36: Estimated Hilbert-Schmidt two-*rebit* separability probabilities for $r_A + r_B = 1$

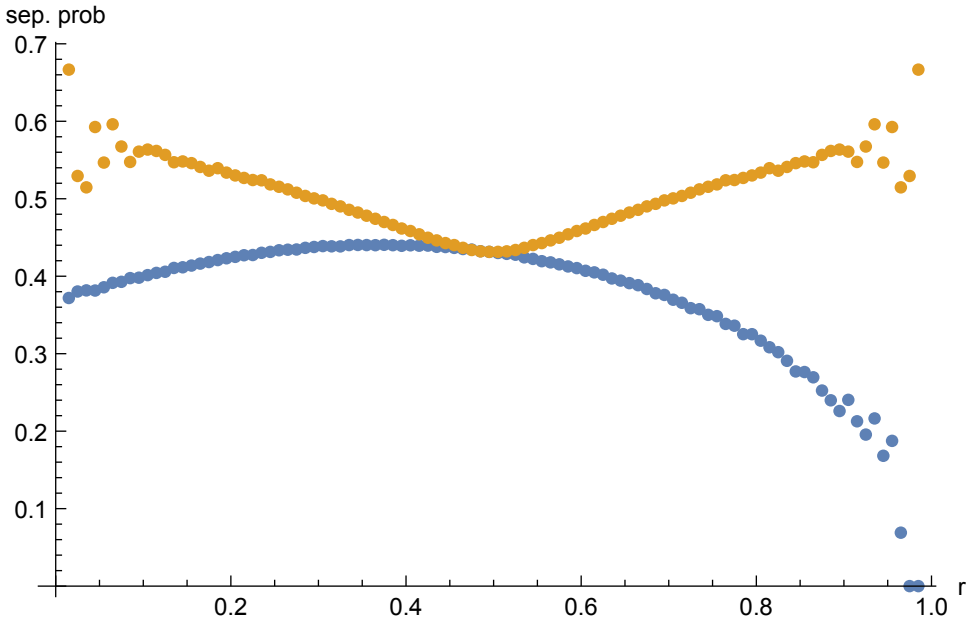


FIG. 37: Joint plot of last two figures

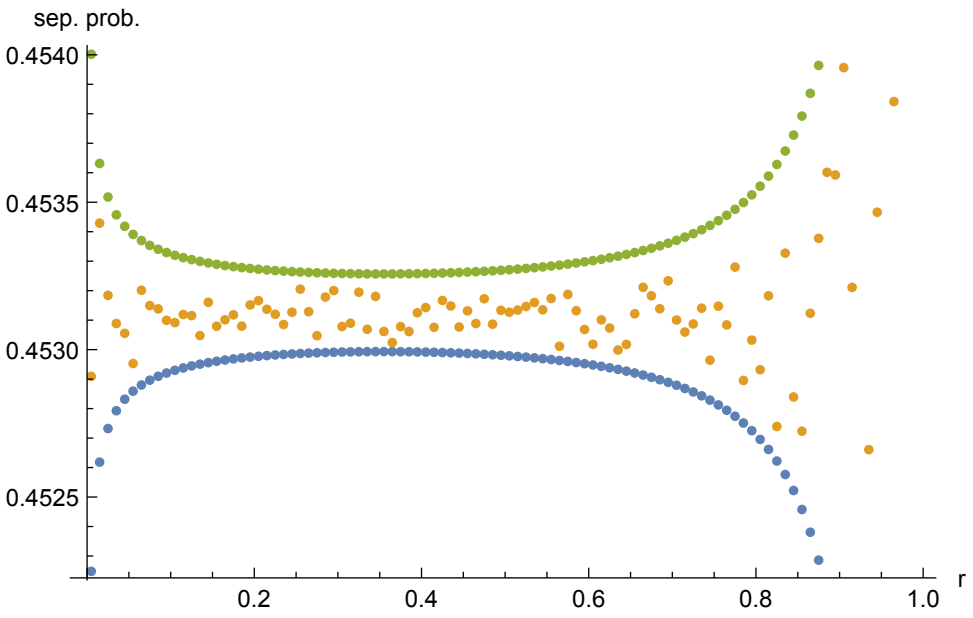


FIG. 38: Estimated (marginal) Hilbert-Schmidt two-*rebit* separability probabilities over either one of the Bloch radii, along with 95% confidence limits about the conjectured value of $\frac{29}{64} \approx 0.4531250$

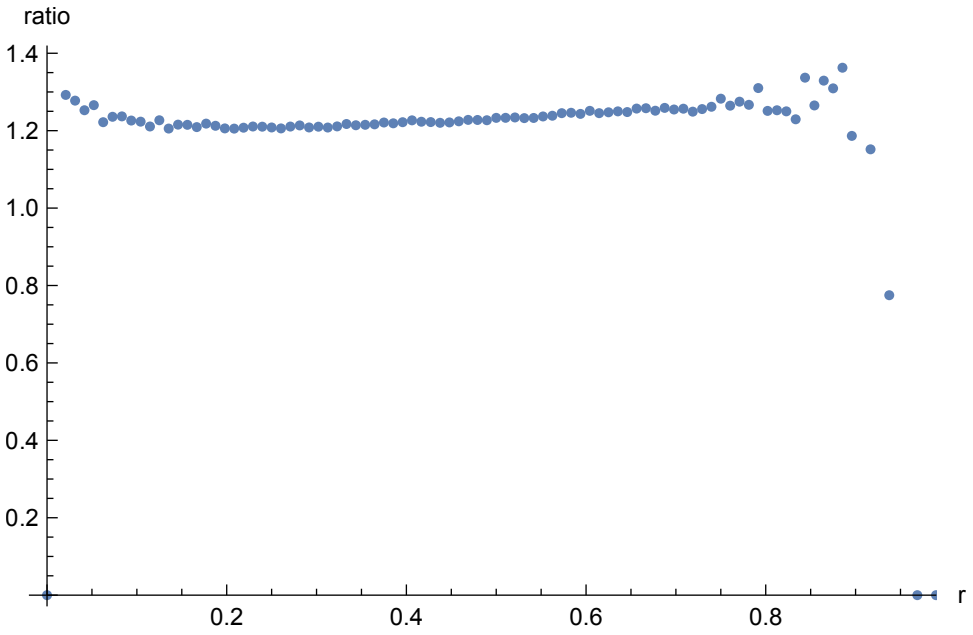


FIG. 39: Ratio of $p^{2-qubit}(r_A = r_B)$ to square of $p^{2-rebit}(r_A = r_B)$

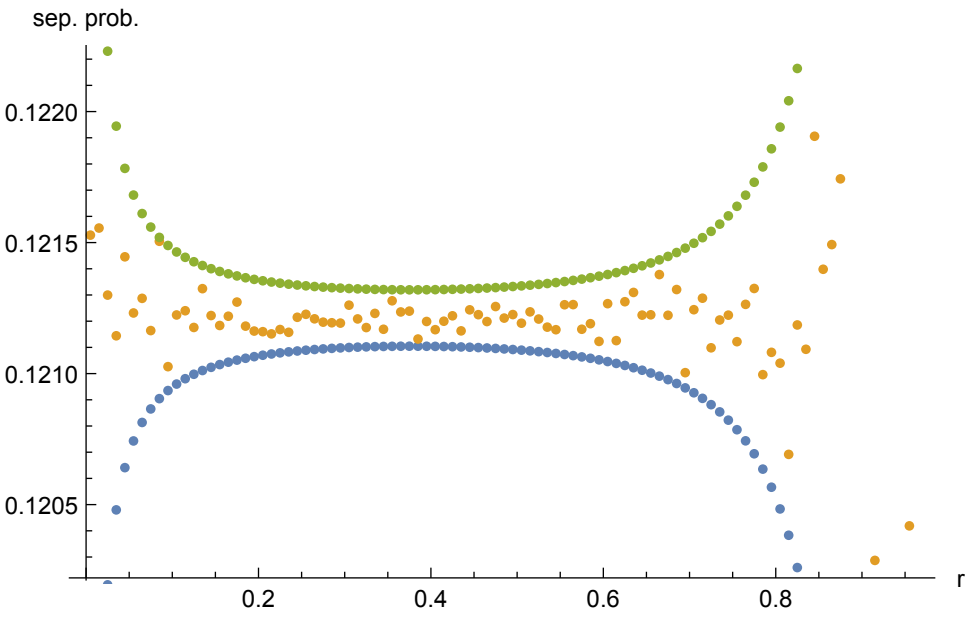


FIG. 40: Estimated two-qubit separability probability for the Hilbert-Schmidt case ($k = 0$) associated with the determinantal inequality $|\rho^{PT}| > |\rho|$, along with 95% confidence limits about $\frac{1}{2}(\frac{8}{33}) = \frac{4}{33} \approx 0.121212$.

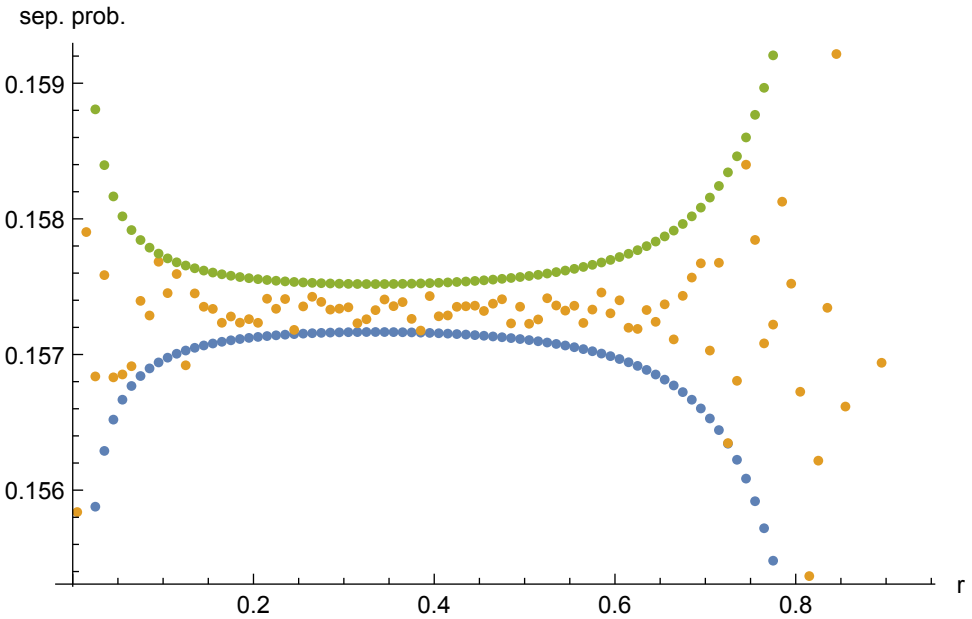


FIG. 41: Two-qubit separability probability for the random induced measure case of $K = 5$ ($k = 1$) associated with the inequality $|\rho^{PT}| > |\rho|$, along with 95% confidence limits about $\frac{45}{286} \approx 0.157343$, with the complementary probability for $|\rho| > |\rho^{PT}| > 0$ being $\frac{61}{143} - \frac{45}{286} = \frac{7}{26} \approx 0.269231$.

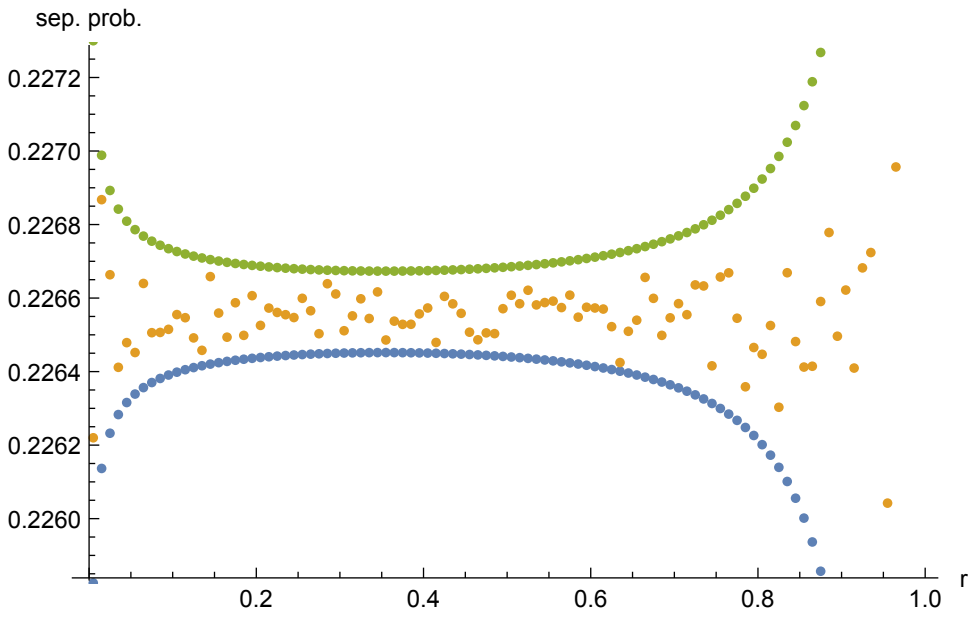


FIG. 42: Two-*rebit* separability probability for the Hilbert-Schmidt case associated with the inequality $|\rho^{PT}| > |\rho|$, along with 95% confidence limits about $(\frac{1}{2})(\frac{29}{64}) = \frac{29}{128} \approx 0.2265625$.

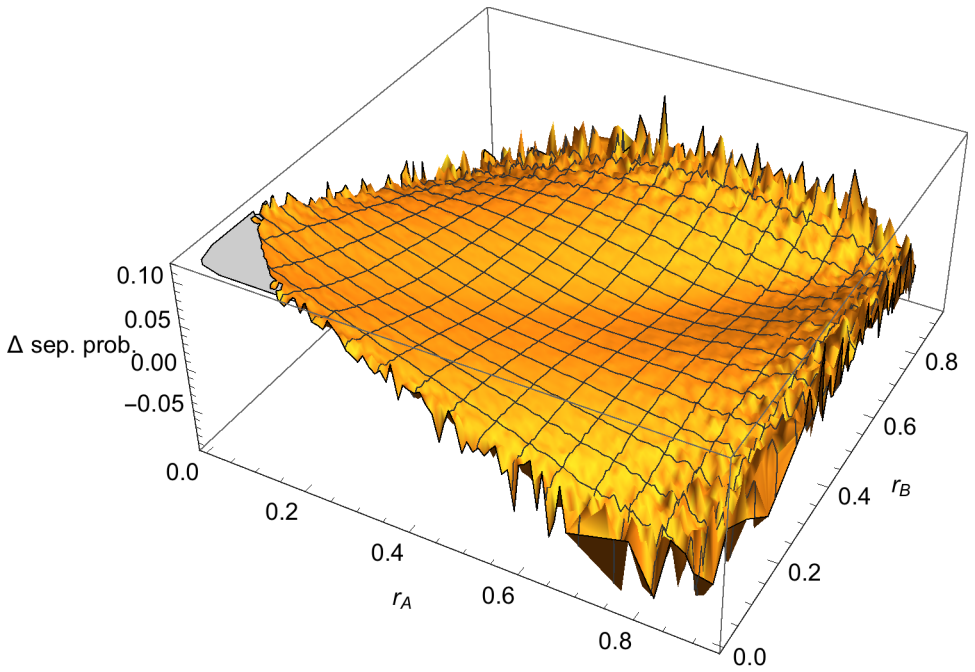


FIG. 43: Residuals of fit of $\frac{8p(r_A,r_B)}{33}$–given by (4)–to the estimated Hilbert-Schmidt two-qubit separability probabilities given in Fig. 5.

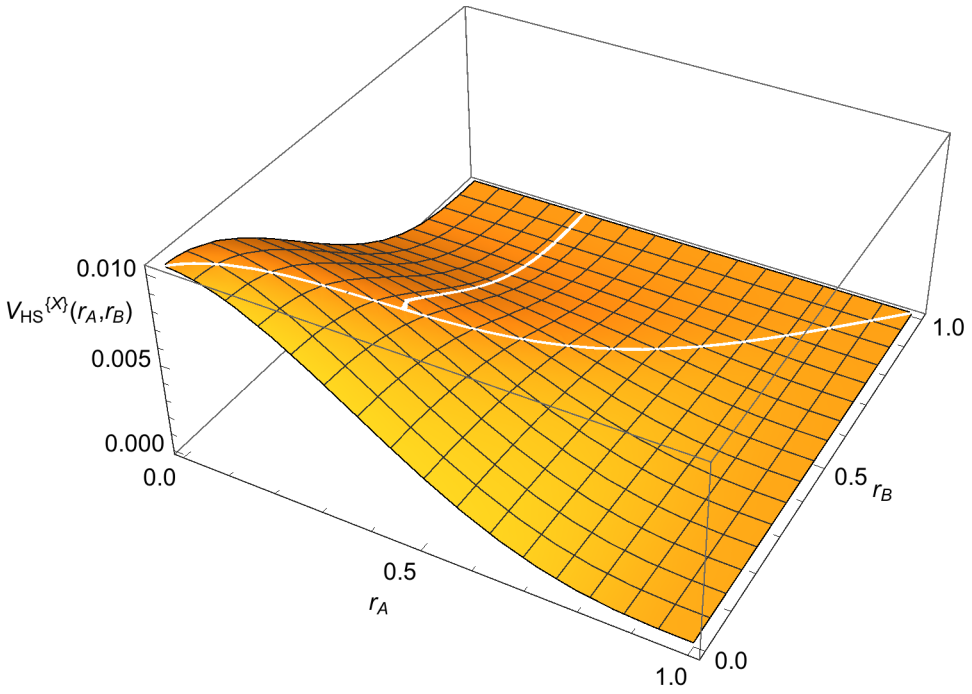


FIG. 44: Bivariate Hilbert-Schmidt volume distribution (9) for the X-state model

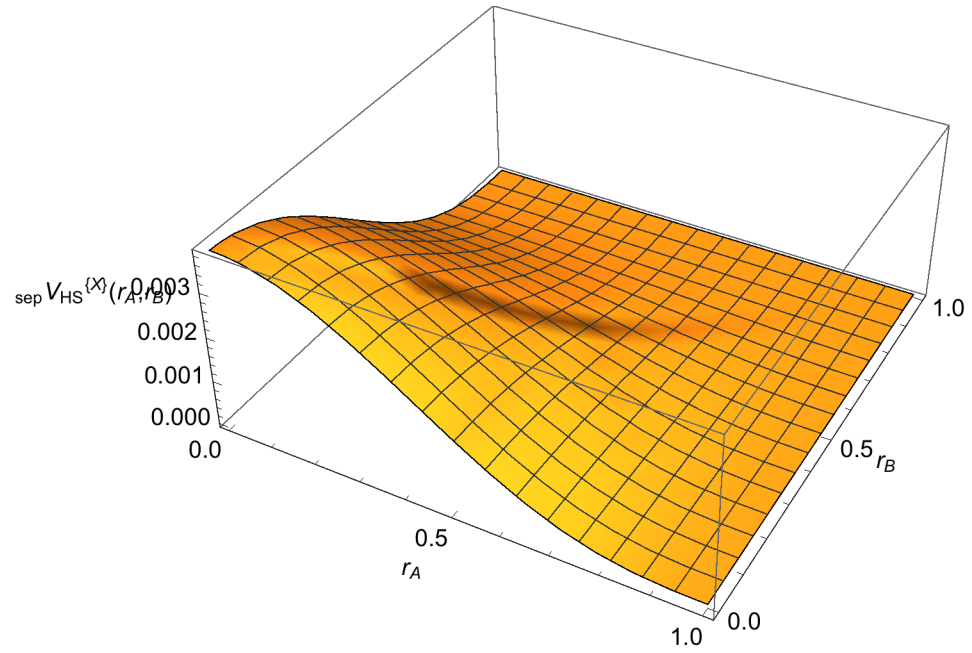


FIG. 45: Bivariate Hilbert-Schmidt *separable* volume distribution (10) for the X-state model

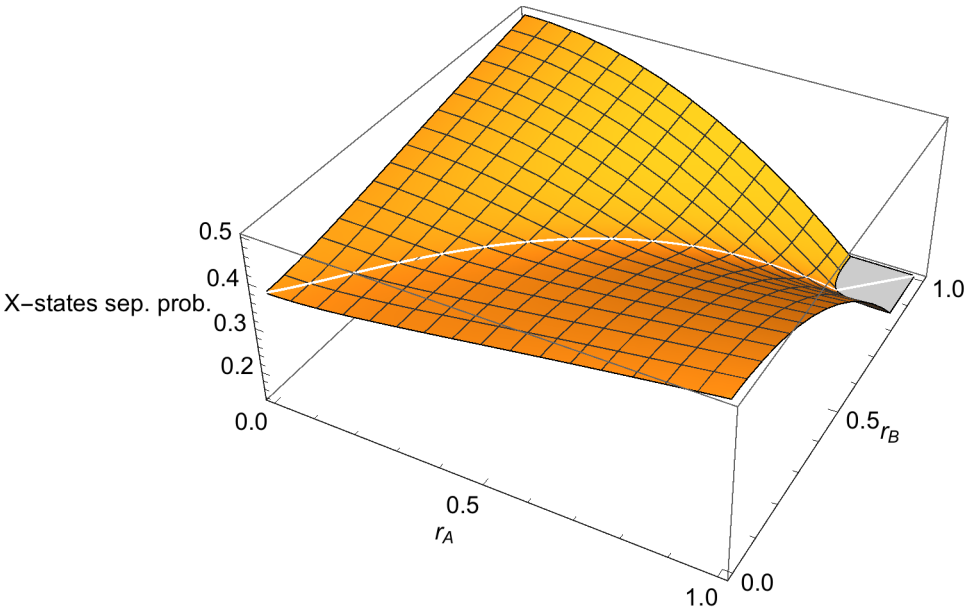


FIG. 46: Bivariate Hilbert-Schmidt separability probability distribution (11) for the X-state model

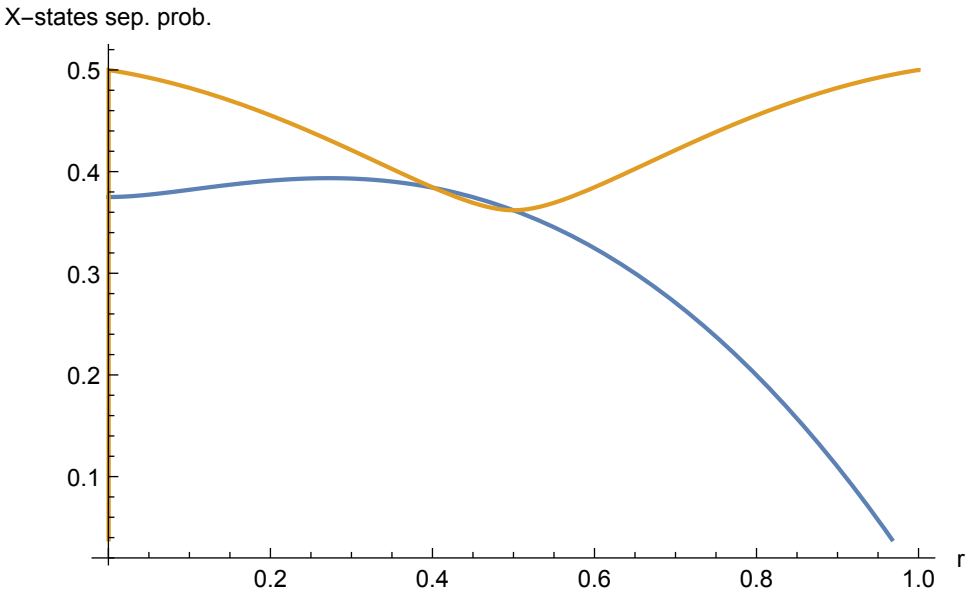


FIG. 47: (Lower) $r_A = r_B$–given by (12)–and (upper) $r_A + r_B = 1$ curves–given by (13)–for bivariate Hilbert-Schmidt X-states separability probability distribution. The minimum of the upper curve is at $r = \frac{1}{2}$, while the maximum of the lower curve is at 0.27227007. In the interval $r \in [0.40182804, \frac{1}{2}]$ the $p^{\{X-states\}}(r_A = 1 - r_B)$ curve is dominated by the $p^{\{X-states\}}(r_A = r_B)$ curve.

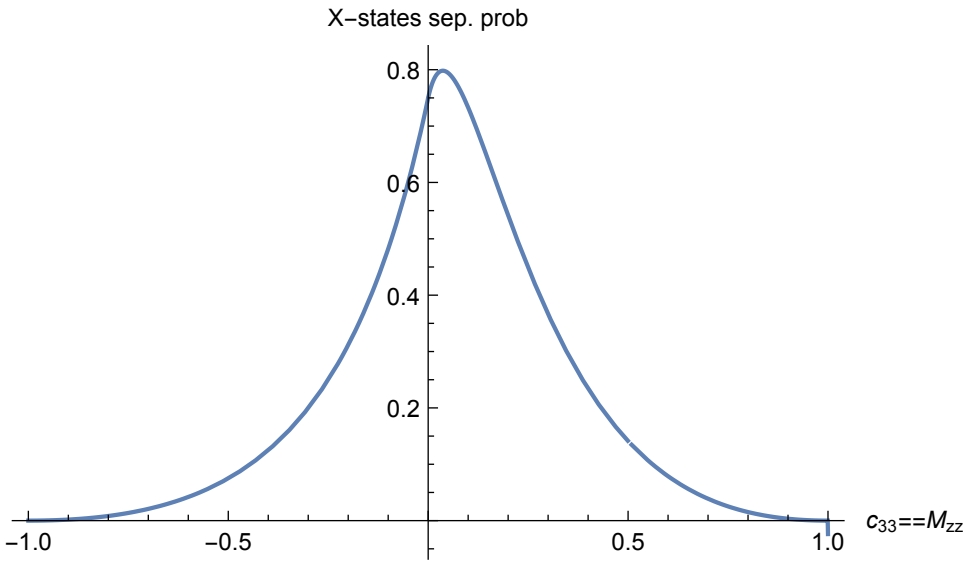


FIG. 48: X-states separability probability as a function of the Fano correlation parameter $c_{33} \equiv M_{zz}$. For $-1 < M_{zz} < 0$, the curve is simply $\frac{3(M_{zz}+1)^2}{2(M_{zz}-2)(2M_{zz}-1)}$. The maximum ($\approx 0.79819147$) occurs near $c_{33} \equiv M_{zz} = 0.03677089$.

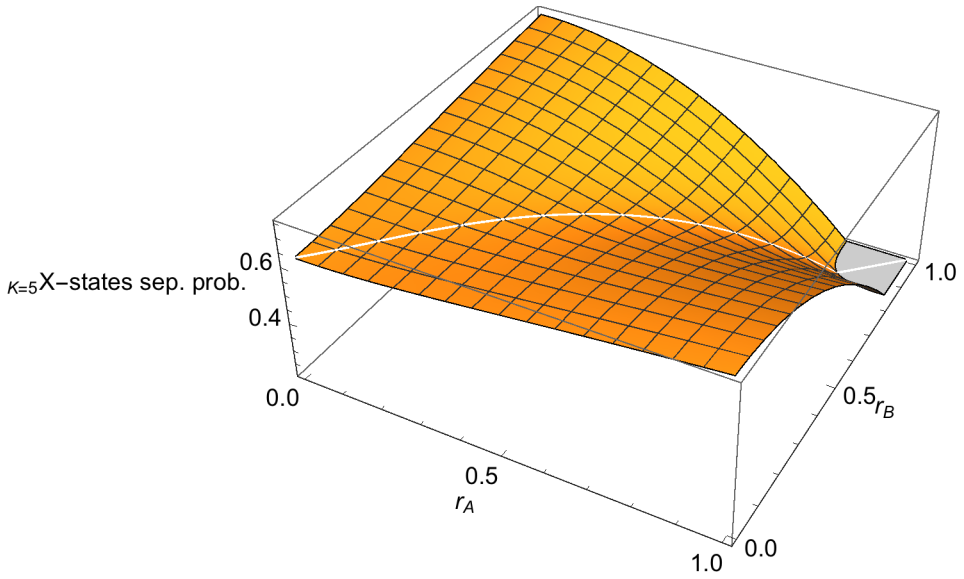


FIG. 49: Bivariate separability probability function for the $K = 5$ induced measure X-states model

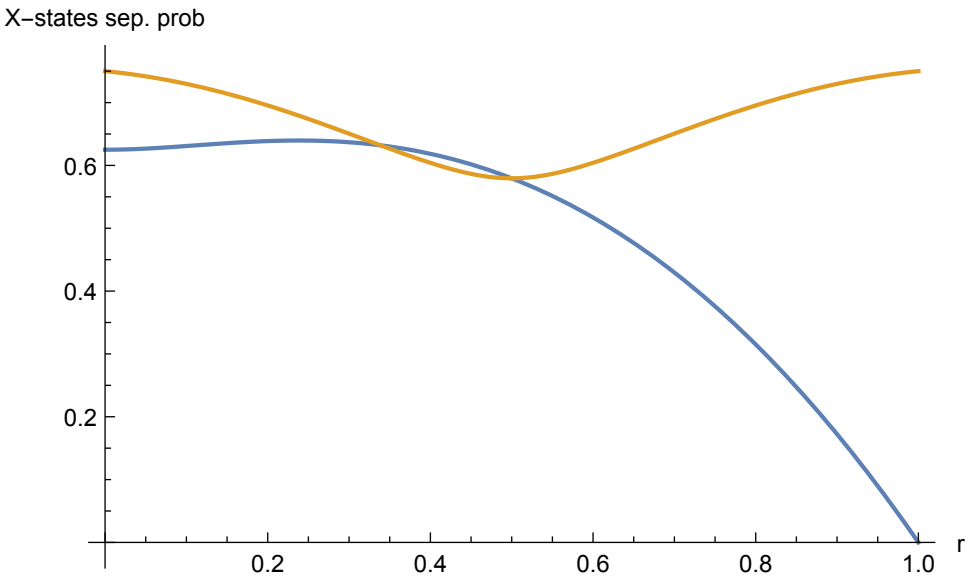


FIG. 50: The $r_A = r_B$ and (largely dominant) $r_A = 1 - r_B$ sections of the $K = 5$ X-states separability probability function (22)

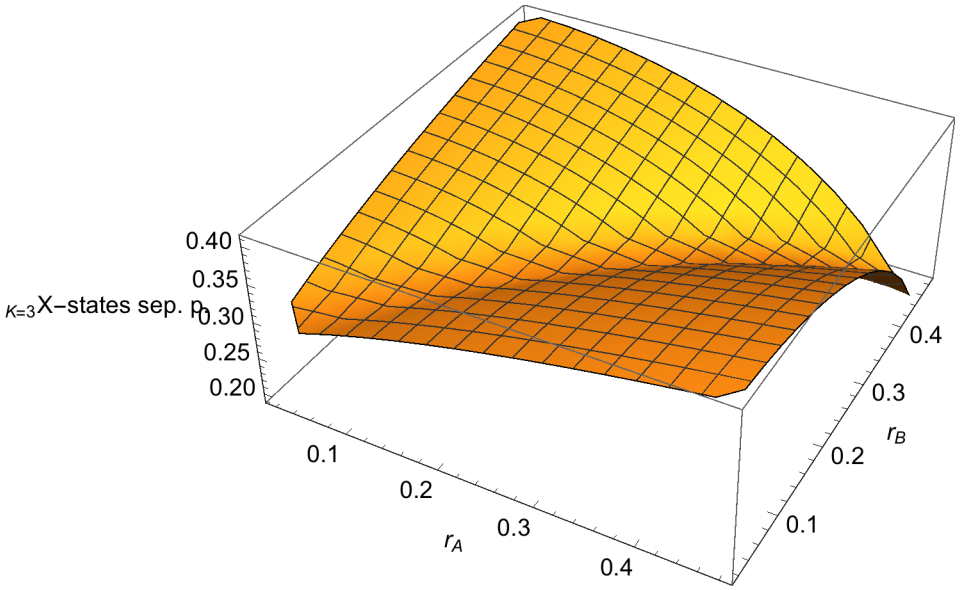


FIG. 51: Numerically-based estimate of bivariate separability probability function for the $K = 3$ induced measure X-states model

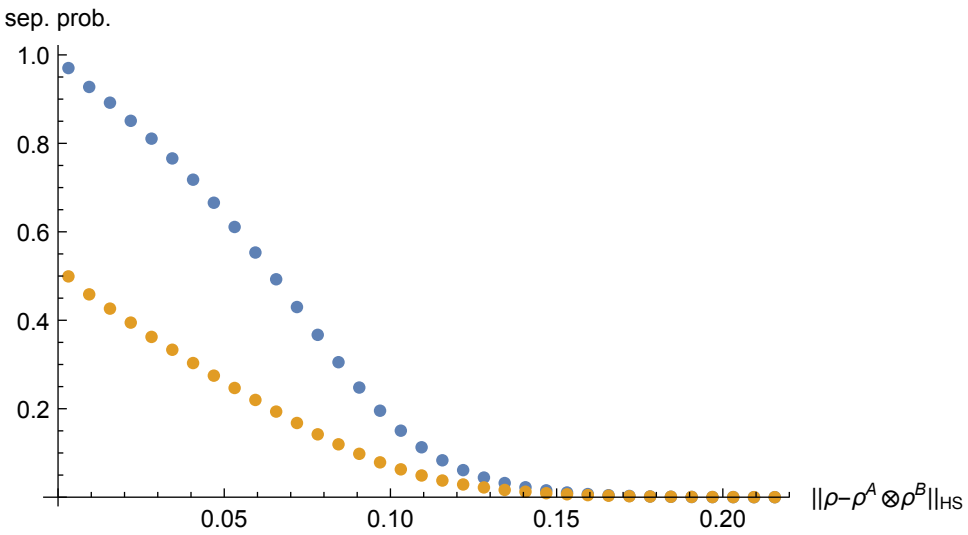


FIG. 52: Two-qubit separability probabilities as a function of the entanglement expression $||\rho - \rho^A \otimes \rho^B||_{HS}$ for the Hilbert-Schmidt (dominant curve) and Bures measures